Final Report
April 1, 1989 - August 31, 1993

THE DYNAMICS OF HYDROPONIC CROPS FOR SIMULATION STUDIES OF THE CELSS INITIAL REFERENCE CONFIGURATIONS

NASA-AMES RESEARCH GRANT No. NCC2-608

Principal Investigator

Tyler Volk

New York University
34 Stuyvesant Street
New York, NY 10003

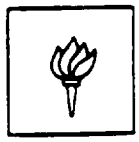

NEW YORK UNIVERSITY

FACULTY OF ARTS AND SCIENCE

DEPARTMENT OF APPLIED SCIENCE

Table of Contents

Introduction

During the past several years, the NASA Program in Controlled Ecological Life Support Systems (CELSS) has continued apace with crop research and logistic, technological, and scientific strides. These include the CELSS Test Facility planned for the space station and its prototype Engineering Development Unit, soon to be active at Ames Research Center (as well as the advanced crop growth research chamber at Ames); the large environmental growth chambers and the planned human test bed facility at Johnson Space Center; the NSCORT at Purdue with new candidate crops and diverse research into the CELSS components; the gas exchange data for soy, potatoes, and wheat from Kennedy Space Center (KSC), and the high-precision gas exchange data for wheat from Utah State University (USU).

All these developments, taken together, speak to the need for crop modeling as a means to connect the findings of the crop physiologists with the engineers designing the system. A need also exists for crop modeling to analyze and predict the gas exchange data from the various locations to maximize the scientific yield from the experiments.

One fruitful approach employs what I and Bruce Bugbee of Utah State University have called the "energy cascade". Useful as a basis for CELSS crop growth experimental design, the energy cascade as a generic modeling approach for CELSS crops is a featured accomplishment in this report. In my opinion, the energy cascade is major tool for linking CELSS crop experiments to the system design. The energy cascade I present here can help collaborations between modelers and crop experimenters to develop the most fruitful experiments for pushing the limits of crop productivity. Furthermore, crop models using the energy cascade provide a natural means to compare, feature for feature, the crop growth components between different CELSS experiments, for example, at Utah State University and Kennedy Space Center.

The Energy Cascade Model

(A version of this work (essentially as presented here, aimed at the CELSS scientists) is being submitted for review to *The Journal of Life Support and Biospheres Studies*, with co-authors Bruce Bugbee and Ray Wheeler. A version with detailed physiology is also under preparation for *The Annals of Botany*.)

SUMMARY OF THE ENERGY CASCADE MODEL

Use of plants in advanced life support (NASA's program in Controlled Ecological Life Support Systems) requires models of crop growth to focus data analysis, to evaluate areas for improvement, and to predict gas exchange properties of crop for design and engineering. We used data from gas exchange experiments at Utah State University and Kennedy Space Center for wheat (Triticum aestivum L.) and examined it for reasonable interpretations of the time-dependence of the major sequence of three components in an energy cascade: photosynthetic photon absorption, canopy quantum yield, and carbon use efficiency. From the Utah State data, we developed a model with a total of five straight lines: absorption increasing during canopy fill, then constant; quantum yield as constant, then decreasing during senescence; carbon use as constant. This system is probably the lower limit of simplicity to which the data can be reduced and yet provide utility. We demonstrated this utility by using the model as developed from the Utah State data to predict gas exchange characteristics for experiments at Kennedy Space Center. The most uncertainty arose in characterizing the canopy quantum yield, especially in predicting a time for the beginning of its senescent decrease. The model should generally be applicable to all crops grown in gas exchange experiments.

INTRODUCTION

To establish a role for plants in advanced life support it is crucial to explore the potential limits of crop productivity. This includes examining the efficiencies of growth, and, for engineering analysis, characterizing the rates of gas exchange of carbon dioxide, oxygen, water vapor, and trace gases. Much research so far has focused on CO_2, because carbon is a keystone element in organic systems, because CO_2 levels are a major control on growth, and because CO_2 exchange is a valuable proxy for monitoring and understanding photosynthesis.

Here we adopt the approach of deconvolving an uppermost suite of components in the production system of plant growth. These are: (1) absorption of photosynthetic photon flux (PPF), characterized as a fraction; (2) conversion of PPF into non-structural carbohydrate (sucrose) during gross photosynthesis, characterized as a canopy quantum yield (moles CO_2 fixed per mole PPF absorbed); and (3) conversion of carbohydrate into the structural and enzymatic portions of plant biomass during net photosynthesis, characterized as a carbon use efficiency (moles CO_2 in biomass per moles CO_2 fixed). Details of these components and estimates of both their theoretical and potentially achievable maxima have been described (Bugbee, 1992a; Bugbee and Monje, 1992).

We call this sequence of components the energy cascade, a series of primary types of conversions of energy. Each step represents an efficiency that can be compared to its potentially achievable value. Our focus here is using the energy cascade as a modeling strategy. Specifically, we use gas exchange data from Utah State University to develop a model. Then we test this model with gas exchange data from Kennedy Space Center. Finally, we tabulate encouraging findings and the key shortcomings and uncertainties that emerge.

THE DATA

The Utah State University (USU) data contain highly-resolved gas exchange rates (averaged over 3-min. intervals), controlled PPF levels,

measured absorbed PPF and area changes, and a minimal scatter in the data during the course of the life cycle of wheat (Monje, 1993). The USU data were collected with a hydroponic growth chamber and continuous monitoring of net canopy uptake of CO_2 during the light hours and net canopy efflux of CO_2 during the dark hours. In addition, root respiration is measured separately at all times. Details of the system and its capabilities have been previously described (Bugbee, 1992b).

Examples of data from the USU system for net photosynthesis, shoot and root respiration, and the computed components of the energy cascade have been explained by Bugbee and Monje (1992). The data we use in this study are from two more recent trials with two different CO_2 levels and all other variables constant (Monje, 1993). Table 1 lists the experimental conditions for the two cases, for low-CO_2 of 330 ppm (henceforth USU1), and for high-CO_2 of 1200 ppm (henceforth USU2).

We also take data from the Biomass Production Chamber at Kennedy Space Center (KSC). These experiments provide gas-exchange values for net photosynthesis and total dark respiration (root and shoot respirations are not separated). The facility and its capabilities for measurements (Wheeler, 1992) and the experiments used in our study, which differ primarily in PPF treatment (Wheeler et al., 1993), have been previously described.

MODEL STRATEGY

Using the energy cascade concept, and terms for gross and net photosynthesis (P_g, P_n), respiration (R), canopy PPF absorption (a), canopy quantum yield (q), and canopy carbon use efficiency (c), we define the following fundamental set of equations:

$$P_g = q\ a\ \text{PPF} \qquad [1]$$

$$P_n = c\ q\ a\ \text{PPF} \qquad [2]$$

$$R = -(1 - c)\ q\ a\ \text{PPF} \qquad [3]$$

With three equations and seven variables (P_g, P_n, R, a , c, q , PPF), four of them must be specified either by measurements or by the model, to compute the others. Normally, the measurements provide P_n, R, a , and PPF—therefore P_g, q, and c are computed:

$$P_g = P_n - R$$

$$q = P_g/(a \text{ PPF})$$

$$c = P_n/P_g$$

For a model, on the other hand, one would want to specify a, q, c, and PPF, and then use Eqs. [1-3] to compute P_g and especially P_n and R for comparison to data. In addition, it is useful to compute the crop growth rate (cgr in g-biomass m^{-2} d^{-1}) and total accumulated biomass (B in g m^{-2}), knowing the photoperiod (h in hours) and a conversion constant (d in g-biomass μmol-CO_2^{-1} s d^{-1})

$$cgr = \frac{d\,(h\ P_n\ -\ (24\ -\ h)\ R)}{24} \qquad [4]$$

$$B = \int_0^t cgr\ dt \qquad [5]$$

MODEL DEVELOPMENT

For the USU data shown in Fig. 1a, the fraction PPF absorption a rises in about 20 days after emergence to near peak values and then slowly declines, due to increased reflectance of the canopy during senescence. The rise is due to canopy fill and closure, which has been modeled as a function of the increasing leaf area index (Charles-Edwards et al., 1986; Goudriaan and Monteith, 1990). The Ceres wheat model (Ritchie, 1991; Ritchie et al.,

unpublished book manuscript) could in principle be used to predict the curve for a, as biomass accumulates and gets partitioned into leaf area.

For our present purposes of uniform simplicity in modeling the components of the energy cascade, we note two major trends in a. One is the nearly-linear increase from initial low values to a maximum. The other is a gradual and slight decrease after the maximum to the end of the life cycle. This senescent decrease plays only a minor role with small changes in a after canopy closure, which we here ignore. We therefore model a with a linear increase and then a constant.

The data for canopy quantum yield q in Fig. 1b for USU1 and USU2 shows complex shapes. Because of significant differences in the early part of the life cycle, the life-cycle average q for the high CO_2 case has a value 1.3 times that for the low CO_2 case. After about day 15, however, the two curves differ by a nearly constant amount, by about 1.25. For a first-order approach to capture the most information with a simple yet physiologically-meaningful concept, we aim to develop a model for the two cases which simply differs by a constant multiple of a generic shape for q. We therefore will use the factor of 1.25 in our model as representative of the effect of CO_2 on canopy quantum yield.

The Ceres wheat model does employ an essentially constant q until the beginning of grain fill (Ceres stage 5), after which senescence causes an approximately linear decrease in q (Ritchie et al., unpublished book manuscript). The simple models of Maas (1993), Goudriaan and Monteith (1990), and Charles-Edwards et al. (1986) assume a constant quantum yield with time. Thus several studies indicate a rather constant quantum yield, at least early in growth. We will do the same, and will ignore some of the enigmatic, non-proportional differences in q between USU1 and USU2 early in the life cycle. These differences are discussed in Monje and Bugbee (1993, in preparation). The consequences of this simplification will appear in the results.

Polynomials could be fit to the data for q, but this would defeat our modeling strategy, because these polynomials would not be significantly simpler than polynomials for the gas exchange properties of P_g, P_n, and R, which exist at a higher order in the system hierarchy than the components

of the energy cascade. If the energy cascade concept is to be useful, we must first try the simplest meaningful form. We choose a constant quantum yield up to a particular point in the life cycle and then a decrease during senescence. From the data for q in Fig 2b, a candidate point for the onset of the decrease is about half way through the life cycle, at anthesis (day 33 in these trials). For simplicity, we assume that q linearly decreases following anthesis to a value somewhat above zero at crop maturity on day 62. In summary, the model for q, like that for a, is two straight lines.

For carbon use efficiency c (Fig. 1c), there are early differences between the high and low CO_2 cases, which we will ignore as second-order effects. Physiological mechanisms for the effect of CO_2 on c are discussed in Bugbee and Monje (1993, in preparation). Like the quantum yield, c decreases. This decline occurs relatively late in the life cycle, and is of secondary importance since it factors into growth rate values that have already become small due to the gradual and earlier decline of q. The dominant pattern in c is constancy over the life cycle. Overall, the similarity between the high and low CO_2 cases is remarkable, and shows that the effect of CO_2 is on the quantum yield (changing the photorespiration), and not on the subsequent dark reactions of carbon use during biosynthesis. In keeping with our strategy of trying to capture most of the pattern with the least amount of effort, we consider c constant over the life cycle.

These deliberations lead to a conceptual system for a, q, and c consisting of a total of five straight lines. Three of the five lines are processes that are constant. The two sloping lines are the periods of increase in a during canopy fill and decrease in q during senescence. Formally, these deliberations lead into a system of equations:

$$a = \left(\frac{a_{max}}{t_a}\right) t \qquad (\text{for } t \le t_a) \qquad [6a]$$

$$a = a_{max} \qquad (\text{for } t \ge t_a) \qquad [6b]$$

$$q = q_{max} \qquad (\text{for } t \le t_q) \qquad [7a]$$

$$q = q_{max} - \left(\frac{q_{max} - q_{min}}{t_m - t_q}\right)(t - t_q) \qquad (\text{for } t \geq t_q) \qquad [7b]$$

$$c = \text{constant} \qquad [8]$$

The terms are fully defined in Table 3.

How well does this model do? First, we will discuss USU1, for low CO_2. We will not dwell on the fit for PPF absorption, because as already indicated, ultimately a might be simulated using a submodel for leaf area as a function of biomass and age. Eq. [6a] assumes that a=0 at t=0, which is approximately valid because first, this is evident in the data, and second, a predicted absorption is only several percent (using the emergence leaf area of 0.4 cm^2/plant from the Ceres-wheat model with the given densities and a Beer's law for absorption). The fitted constants in Eqs. [6a,b] for USU1 (a_{max} and t_a) are given in Table 2.

To compute q in Eqs. [7a,b], we take q_{max} from the stable, relatively high values of q between about 15 and 30 days of USU1 (see Fig. 1b). As described further below, the Ceres wheat model predicts a phenology with constant temperatures in which anthesis occurs at about 0.52 t_m (t_m = time of maturity. Therefore, we take $t_q = 0.52\ t_m$, which returns t_q = 32 days, one day off the actual value of 33 days. After t_q, q declines, and we use a line that approximately gives the same average as the data for q during the interval between t_q and t_m. We use a final value of q (q_{min}) equal to 0.2 q_{max}.

For the carbon use efficiency c, we fit the data between about days 15 and 45, ignoring secondary details during the early, more potentially problematic behavior and during the later senescence of carbon use. The constant we use is c = 0.68.

With these calibrations for a, q, and c (See Fig. 1) and the PPF data as noted in Table 1, we use Eqs. [6-8] in Eqs. [2-4] to compute P_n, R, and cgr. (We do not show P_g, since this is simply derived from P_n and R) The results in Fig. 2 for P_n, R, and cgr look quite good for USU1. But of course, the modeling to this point has been circular, since data led to

calibrated values for the constants, which then merely led back to the same data. Nevertheless, judgments were made to ignore what at times in the life cycle are significant discrepancies, and therefore the comparison between our simple model and the gas exchange data is still instructive.

As we move to the high CO_2 case of USU2, as described above we set the quantum yield ratio to 1.25. Therefore, q_{max} and q_{min} for USU2 equal, respectively, 1.25 q_{max} and 1.25 q_{min} for USU1. All other parameters of the model carry over from the calibrations of USU1.

Results for the USU2 case are also shown in Figs. 1 and 2, and again, these results look encouraging. Our model is reasonable, simple, and consists of parts each explainable by a physiological process, which makes them conducive to more elaborate formulations, should these needs arise. However, we must be wary still of a certain circularity in the approach. The results for P_n, R, and cgr are valuable for insight into how well the interpretation for a, q, and c with five straight lines mimics the general shapes and trends of the gas exchange data, but we would be surprised at any large discrepancies, since judgements about how to model a, q, and c were made with an eye to the data for both USU1 and USU2. So far this model is a helpful tool for analysis, but not really predictive. For that, we turn to the gas exchange data from Kennedy Space Center.

MODEL TESTING

The KSC experiments differ from those of USU in cultivar, hydroponic technology, CO_2 level, temperature, and PPF. We will assume the following: (1) The different PPF level will be a major controlling input to the model (Bugbee and Salisbury, 1988); (2) The KSC CO_2 level is very close to saturation (Wheeler et al., 1993), like the USU2 CO_2 level. Therefore the USU2 parameters q_{max} and q_{min} will apply for KSC1 and KSC2; (3) Having no information otherwise, we assume the hydroponic treatment is not a variable; (4) Given that both sites aim for unstressed conditions, the carbon use efficiency may be the same; and, (5) the phenology of the KSC cultivar, Yecora Rojo, will be predominantly a function of photoperiod and temperature (Volk and Bugbee, 1991). This is

important, for we need to use a development model to predict the switch times t_q and t_m, given the different temperature treatments.

The USU and KSC experiments all used a photoperiod of 20 h, which is the value at and above which this component of development is a maximum in the Ceres wheat model (Ritchie (1991). Therefore we need only consider the thermal time component of development. Bugbee and Salisbury (1988) grew the KSC cultivar Yecora Rojo under a temperature treatment nearly the same as the KSC experiments (daily thermal time average of 19.17 ^{o}C-d, compared to 19.63 for KSC1 and 19.48 for KSC2). The larger daily thermal time for KSC should slightly reduce the time to maturity of 79 days found by Bugbee and Salisbury to (19.17/19.63)(79)=77 days and (19.17/19.48)(79)=78 days, respectively, for KSC1 and KSC2.

From the development routines in the Ceres wheat model (Ritchie, 1991), assuming constant temperature during the life cycle and a phyllochron of 85 ^{o}C-d leaf^{-1}, the ratio of the time from emergence to anthesis compared to the time from emergence to maturity is 0.52. Were the DTT constant, anthesis for KSC1 and KSC 2 would be predicted at 0.52(78)=41 and (0.52)77=40 days, respectively. (Using other typical phyllochron values discussed by Ritchie would only affect these estimates by a couple days, and not alter the conclusions to our model.) However, because the early days were warmer (see Table 1 notes), the anthesis must be shortened by about 3 days in KSC1 and 1 day in KSC2 from that predicted by the above ratio. For simplicity, we treat both cases the same and assume t_m = 78 d and t_q = 39 d.

With these predictions for the times, only a single parameter needs to be formally chosen from the actual KSC data. Canopy closure must be shortened (see Fig. 3a), and we decrease t_a from 12 days in the USU models to 9 days for the KSC models. (Note the KSC density is about double.)

All other parameters needed for the KSC models are the same as those developed for the USU models.

Figures 3 and 4 show the models results for the two cases of PPF levels in KSC1 and KSC2 (explained in the notes to Table 1).

In several ways we judge the model to be a success. The good representation for PPF absorption in Fig. 3a is expected, since the time to closure, t_a, was adjusted to compensate for the higher planting density of the KSC experiments. Uncertainty about the PPF reflected from the substrate during the canopy fill period makes it impossible to speak more quantitatively about the fit, other than that the two straight lines seem adequate. Also, the a_{max} from the USU models used as a constant for a during most of the life cycle works in the KSC data as well; in other words, the decrease of a during senescence is slight and only a secondary event in the context of the entire energy cascade.

Regarding the canopy quantum yield in Fig. 3b, we have chosen not to compute data for q from the KSC experiments because of uncertainty in a during the early canopy fill already discussed, and because of uncertainties (elaborated upon more in the discussion section below) about how to incorporate changing PPF levels during the experiments, about changing growth areas during the experiments, and in general, limitations from the larger scatter in the gas exchange data in the KSC experiments. Since data for q would in any case be derived from the gas exchange data, the general strategy is to use our model for a, q, and c to predict the gas exchange values, and thus we can go directly to them to judge the adequacy of the model.

Fig. 3c shows that the KSC data for carbon use efficiency is somewhat higher (average about 0.7) than the model value c=0.68 developed for the USU models. This difference is relatively unimportant, and the similarity is encouraging. Our judgement seems valid that in a simple model of the energy cascade, c can be taken as a constant.

Turning to the comparison between models and data for P_n, R, and cgr in Fig. 4, we see that the models capture the general magnitudes of the data, getting to within about 10% of the average peak plateaus for P_n and cgr in KSC1 and KSC2. The downward trend in q due to senescence is exhibited by the data. In KSC1, dimming of the lamps at day 24 after emergence decreased the P_n and cgr, and our model captures this change well, especially if one compares the difference between average peak values before and after the dimming to the model's predicted difference. Finally,

the time of physiological maturity based on temperature predictions from the Ceres model is close to that in the data. The model's t_m is about 3-4 days too short compared to the data, but this is acceptable given the difficulties with crop phenology predictions for cultivars without a large data base.

In other ways, the comparison between model and data in Fig. 4 points to shortcomings. Most significantly, we note: the beginning of senescence in the model overshoots the actual point in the data. This is most clearly seen in KSC2, and results in a large (about 20%) overprediction in the P_n and *cgr* between days 30 and 50. Also, the model's senescence, as in the USU cases, would clearly work better if it were formulated as a curve, rather than as a line.

Overall, the model appears successful, given the absence of additional fitting when applied to the KSC data. The magnitudes of the gas exchange measurements are simulated, which vary by about a factor of 2 between the USU and KSC experiments, as are the general trends of increase, plateau, and senescence.

DISCUSSION

This paper is meant to present a simple model to provide a basis for a more rigorous comparison of data sets with relatively comparable gas exchange measurements. The model is as useful for a physiologically-based process of analysis, as it is for prediction. The energy cascade built from the simple trends avoids an analysis getting lost in a jungle of polynomials that can go no further than individual fits.

Polynomial fits with standard statistical measures would obviously produce higher correlations than we show. But an often more important—if sometimes less tangible—aspect of a model is its usefulness in incorporating terms that have physiological meaning (Volk and Bugbee, 1991). Such a model, when suitably simple, often prevails because it can serve as a solid base for additional development. Furthermore, a model needs to suit the type of data: we question whether more detailed modeling would be served in this case. For example, note that during the first 20

days the two KSC experiments differ to a greater degree in the data than in the models (KSC1 with lower values for P_n than KSC2), which, given the similarity in environmental conditions between the two experiments during the early part of life cycle, we attribute to lack of exact replication in the experiments, a common problem of crop growth experiments with canopies.

One further numerical evaluation of the model can be presented. For all four experiments, the *cgr* has been integrated using Eq. [5] to show in Fig. 5a the total biomass *B* and in Fig. 5b the difference between the modeled *B* and actual *B* (Fig. 5b) for all four experiments from USU and KSC. Fig. 5a shows the dramatic differences among the experiments in the magnitudes of *B* and in the durations of the life cycle, all of which are modeled reasonably well.

Focusing on the differences between models and data in Fig. 5b, and focusing on the time of substantial biomass after about day 20 in all cases, we note that the USU models for *B* always differ less than 10% from their data, and the KSC models vary by less than 15% from their data. We can see that the models for KSC produce values larger than the data, while the USU models are less than the data. These discrepancies emphasize again that the canopy quantum yield for KSC should be smaller than that taken from USU2, rather than the same. However, we have not fit this term, and based it solely on the similarities of CO_2 between USU2 and the KSC trials. At physiological maturity all four models end with an error of about 6% or less.

Our model can serve as a heuristic device for formulating further questions based on the inadequacies. In our opinion, the most outstanding are as follows.

In the future we could examine how well our specified PPF absorption *a* could be replaced with a Beer's Law formulation based on a leaf area index from biomass partitioning (for example, see Maas, 1993; Goudriaan and Monteith, 1990; Charles-Edwards et al., 1986; Ritchie et al., unpublished book manuscript). However, the gains would have to weighed against the added complexity in parameters.

There are numerous issues about the canopy quantum yield raised by our study. Perhaps primary among them is the need for precise area measurement of the crop to compute well-constrained values for q from the gas exchange data. This is not a trivial measurement in controlled environments, and is usually confounded by 'side' lighting. Measurements during the USU experiments indicate the area increased from about 0.7 m^2 at planting to about 1.1 m^2 in the fully developed canopy. This was accounted for in the computations. A similar increase may have occurred during the KSC experiments, for which we have used an estimated average value. This is likely to be the largest uncertainty in any putative computation of the KSC values for q.

Furthermore, the unknown area changes in the KSC experiments is probably to some extent compensated by the PPF level that gradually increased as the plants grew closer to the lamps. The satisfactory predictions in the magnitudes of gas exchange for the KSC experiments, therefore, may contain two compensating variables that each might affect the calculations by several tens of percent. This is an area for more work.

Another future issue is concerns a linear vs. non-linear dependence of P_n on PPF. The linear case is what we have assumed; in other words, q = constant. This has shown to be a good assumption in experiments at KSC during which *PPF* is lowered by degrees from its peak level of nearly 800 $\mu mol\ m^{-2}\ s^{-1}$ (Wheeler et al., 1993), and in similar, short term experiments at USU up to nearly 2000 $\mu mol\ m^{-2}\ s^{-1}$ (Meek, 1990).

Considering field data, for example, we have fit a line to the canopy quantum yield data for wheat at different PPF levels presented by Norman and Arkebauer (1991a, p. 88). This fit would predict that the q from the KSC experiments would have been 20-30% larger than the q at USU. Similar numbers can be derived from the controlled environment experiments of Bugbee and Salisbury (1988). Because our model compares so well to the KSC data, we do not see this effect. Perhaps the area uncertainty is a compensating factor here too, which masks seeing more detail in the canopy quantum yield. One possibility is using canopy models to investigate the issues of canopy quantum yield as a function of PPF, with parameters set for the growth chamber wheat. Possible models to consider

are the CUPID model of Norman and Arkebauer (1991a,b; note our q is their "light-use efficiency"), Sinclair's two-layer model (1991, note our q is his "radiation-use efficiency"), Acock's model (1991), the models summarized by Boote and Loomis (1991), and the integrated model of Norman (1993), which may be particularly appropriate for the diffuse PPF of the growth chamber.

Another area for further work is the term t_q, the onset of senescence in our model. Setting t_q around anthesis works for the USU data but is too late for the KSC data. This may be due to the elevated ethylene levels in the 'closed' Biomass Production Chamber at KSC. Ethylene, along with other organic volatiles present in the KSC experiments, affect the development events (Wheeler et al., unpublished). The smaller root zone depth in the KSC hydroponic system, compared to USU, could be a factor. We also note that in the Ceres wheat model (Ritchie at al., unpublished book manuscript), the decline in quantum yield begins even later than in our model, at the beginning of grain fill.

Definitively characterizing q during canopy fill remains an issue that needs to be investigated with more detailed models. Our work helps highlight some of the questions about the constancy (or inconstancy) of q up until the onset of senescence.

We have ignored temperature effects on quantum yield. However, the temperature differences between the USU and KSC experiments were not great (although they do affect phenology significantly, as we have shown), and considering the potential for adaptation to flatten the effects shown by short term experiments (Meek, 1990), temperature effects are probably minor compared to the role of PPF and the uncertainties in other processes discussed above. Again, more work here would be useful.

We have not specifically derived a saturation curve for q as a function of CO_2, although it could be done. This was not necessary because the q required for the KSC experiments was taken from the USU2 case of high CO_2.

CONCLUSIONS

This paper presents a simple model that has demonstrated utility in the predictions of gas exchange for wheat canopies.

We believe the model could serve as a first-order approximation for gas exchange during the life cycle, as required by the engineers in the NASA Program in Controlled Ecological Life Support Systems (CELSS). They need models for design tradeoffs with light and temperature controls. The gas exchange predictions would be helpful at this current early stage of CELSS design, for sizing system components for planned experiments, for example, for the CELSS Test Facility on the space station and for the human-occupied test bed planned at NASA's Johnson Space Center. The model also has utility by forcing comparisons between different gas exchange data sets which might not otherwise be made. By predicting data, the assumptions about the underlying processes of the energy cascade can be tried and evaluated.

We hope for some originality. Simple canopy models (for a summary, see Boote and Loomis, 1991) can compute a PPF absorption and a canopy quantum yield. But we specifically have shown that a senescence term, like those used in the detailed field crop models (Ritchie et al., unpublished book manuscript; K. Boote, 1992, personal communication) is appropriate for such simple models. Furthermore, we have incorporated an additional important term to the energy cascade by examining the carbon use efficiency.

We have made judgments on the behaviors of the components of the energy cascade that we expect will lead to further model developments and guide experimental design by highlighting areas of uncertainty and periods during the life cycle that deserve special special attention. For example, if theoretical considerations suggest that we cannot improve q_{max}, perhaps attention should focus on the later part of the life cycle and on improving q_{min}.

We suspect the model could be usefully applied to other crops, such as the gas exchange experiments from potatoes and soybeans at KSC, and thus serve as a general modeling platform for analysis and prediction.

ACKNOWLEDGMENTS

We thank John Norman for his unabated attention that helped carry along a three-hour presentation of this material at Utah State University on March 7, 1993. We also thank Oscar Monje and Kenneth Corey for their respective efforts at USU and KSC.

REFERENCES

Acock, B. 1991. Modeling canopy photosynthetic response to carbon dioxide, light interception, temperature, and leaf traits. In Modeling Crop Photosynthesis—from Biochemistry to Canopy, CSSA Special Publication No. 19. Editors K.J. Boote and R.S. Loomis. 41-55.

Boote, K.J., and R.S. Loomis. 1991. The prediction of canopy assimilation. In Modeling Crop Photosynthesis—from Biochemistry to Canopy, CSSA Special Publication No. 19. Editors K.J. Boote and R.S. Loomis. 109-140.

Bugbee, B. 1992a. Determining the potential productivity of food crops in controlled environments. Advances in Space Res. 12: (5)85095.

Bugbee, B. 1992b. Steady-state canopy gas exchange: system design and operation. HortScience. 27: 770-776.

Bugbee, B., and O. Monje. 1992. The limits of crop productivity. BioScience. 42: 494-502.

Bugbee, B., and F.B. Salisbury. 1988. Exploring the limits of crop productivity I. Photosynthetic efficiency of wheat in high irradiance environments. Plant Physiol. 88: 869-878.

Charles-Edwards, D.A., D. Doley, G.M. Rimmington. 1986. Modeling Plant Growth and Development. Academic Press, Sydney.

Corey, K.A. 1989. Dynamics of carbon dioxide exchange of a wheat community grown in a semi-closed environment. NASA/ASEE Summer Faculty Fellowship Program 1989 Research Reports, CR-166837. Editors E.R. Hosler and D.W.Armstrong. NASA John F. Kennedy Space Center. 58-84.

Corey, K.A., and R.M. Wheeler. 1992. Gas exchange in NASA's biomass production chamber. BioScience. 42: 503-509.

Goudriaan, J., and J.L. Monteith. 1990. A mathematical function for crop growth based on light interception and leaf area expansion. Annals of Botany. 66:695-701.

Maas, S.J. 1993. Parameterized model of gramineous crop growth: I. leaf area and dry mass simulation. Agron. J. 85:348-353.

Meek, D.B. 1990. The relationship between leaf area index and photosynthetic temperature response in wheat (*Triticum* aestivum L.) canopies. M.S. thesis. Utah State Univ., Logan.

Monje, O.A. 1993. Effects of elevated CO_2 on crop growth rates, radiation absorption, canopy quantum yield, canopy carbon use efficiency, and root respiration of wheat. M.S. thesis. Utah State Univ., Logan.

Monje, O.A. and B. Bugbee. 1993 (in preparation). Effects of elevated CO_2 on crop growth rates, radiation absorption, canopy quantum yield, canopy carbon use efficiency, and root respiration of wheat.

Norman, J.M. 1993. Scaling processes between leaf and canopy levels. In Scaling Physiological Processes: Leaf to Globe. Edited by J.R. Ehleringer and C.B. Field. 41-76.

Norman, J.M., and T.J. Arkebauer. 1991b. Predicting canopy photosynthesis and light-use efficiency from leaf characteristics. In Modeling Crop Photosynthesis—from Biochemistry to Canopy, CSSA Special Publication No. 19. Editors K.J. Boote and R.S. Loomis. 75-94.

Norman, J.M., and T.J. Arkebauer. 1991a. Predicting canopy light-use efficiency from leaf characteristics. *In* Modeling Plant and Soil Systems—Agronomy Monograph no. 31. Editors J. Hanks and J.T. Ritchie. 125-143.

Ritchie, J.T. 1991. Wheat phasic development. *In* Modeling Plant and Soil Systems—Agronomy Monograph no. 31. Edited by J. Hanks and J.T. Ritchie. 31-54.

Ritchie, J.T., D.C. Godwin, and S. Otter-Nacke. No date. Ceres-wheat: a Simulation Model of Wheat Growth and Development. Unpublished book manuscript.

Sinclair, T.R. 1991. Canopy carbon assimilation and crop radiation-use efficiency dependence on leaf nitrogen content. In Modeling Crop Photosynthesis—from Biochemistry to Canopy, CSSA Special Publication No. 19. Editors K.J. Boote and R.S. Loomis. 95-107.

Volk, T., and B. Bugbee. 1991. Modeling light and temperature effects on leaf emergence in wheat and barley. Crop Sci. 31:1218-1224.

Wheeler, R.M. 1992. Gas-exchange measurements using a large, closed plant growth chamber. HortScience. 27: 777-780.

Wheeler, R.M., K.A. Corey, J.C. Sager, and W.M. Knott. 1993. Gas exchange characteristics of wheat stands grown in a closed, controlled environment. Crop Sci. 33:161-168.

Table 1. Crop growth parameters for experiments from Utah State University (USU1, USU2) and Kennedy Space Center (KSC1, KSC2)

Condition	USU1	USU2	KSC1	KSC2
PPF [a]	1400	1400	550	690
CO_2 (μatm)	330	1200	1000	1000
T (day/night) [b]	23/23	23/23	20.2/16.8	20.1/16.4
Plants m^{-2}	700	700	1500	1500
Area (m^2) [c]	1.0	1.0	20.0	20.0
Cultivar	Veery-10	Veery-10	Yecora Rojo	Yecora Rojo

[a] The PPF (μmol m^{-2} s^{-1}) at USU was 300 between days 0 to 1.5, 800 between days 1.5 to 8, and thereafter 1400. PPF averages for KSC are from Wheeler et al. (1993). KSC1 had a special event: we use a PPF of 660 until dimming of the lamps to about 500 at day 24 after emergence.

[b] Temperatures for KSC1 were 23 °C for the first 20 days after planting, 20 °C until day 33, then 20 °C/16 °C (light/dark) for the remainder. Temperatures for KSC2 were 23 °C for the first 10 days after planting, then 20 °C/16 °C (light/dark) for the remainder.

[c] Areas for USU1 and USU2 were measured during the life cycle, increasing from 0.7 to 1.1.

Table 2. Model parameters for experiments from Utah State University (USU1, USU2) and Kennedy Space Center (KSC1, KSC2)

Parameter	USU1	USU2	KSC1	KSC2
a_{max}	0.93	— [a]	—	—
t_a	12	—	9	—
q_{min}	0.2 q_{max}	1.25$q_{min,USU1}$	—	—
q_{max}	0.05	1.25$q_{max,USU1}$	—	—
t_q	0.52 t_m	—	0.52 t_m - 2 [b]	—
t_m	62	—	78	—
c	0.68	—	—	—

(a) "—" means the same value as to the left on the same row.

(b) See text for explanation.

Table 3. List of symbols

Symbol	Name	Units
a	fraction PPF absorbed by canopy	non-dimensional
a_{max}	fraction PPF absorbed after $t=t_a$	non-dimensional
B	accumulated biomass	g m^{-2}
c	carbon use efficiency	mol biomass-C/mol fixed-CO_2
cgr	crop growth rate	g m^{-2} d^{-1}
d	conversion constant = 2.35	g-biomass s µmol-CO_2^{-1} d^{-1}
h	photoperiod	h
PPF	photosynthetic photon flux	µmol m^{-2} s^{-1}
q	canopy quantum yield	mol-CO_2-fixed/mol-PPF
q_{min}	canopy quantum yield at $t=t_m$	mol-CO_2-fixed/mol-PPF
q_{max}	canopy quantum yield until $t=t_q$	mol-CO_2-fixed/mol-PPF
t	time	d
t_a	time-switch for behavior of a	d
t_q	time-switch for behavior of q	d
t_m	time at crop maturity	d
T	growth chamber temperature	^oC

Figure Captions

Fig. 1. (a) PPF absorption a, (b) canopy quantum yield q, and (c) carbon use efficiency c for USU1 and USU2 data and models, plotted as days after emergence.

Fig. 2. (a) Net photosynthesis P_n and respiration R, and (b) crop growth rate cgr, for USU1 and USU2 data and models, plotted as days after emergence.

Fig. 3. (a) PPF absorption a, (b) canopy quantum yield q, and (c) carbon use efficiency c for KSC1 and KSC2 data and models, plotted as days after emergence. Data for q were not computed due to uncertainties described in the text. The bars of uncertainty during canopy fill for a (only taken during KSC2) brackets data between a lower bound calculated by Corey (1989), without a measured reflected flux from the substrate back up into the canopy, and our computed upper bound, calculated by assuming an albedo for the substrate of 0.7, approximately that of the hydroponic growth trays at USU.

Fig. 4. (a) Net photosynthesis P_n and respiration R, and (b) crop growth rate cgr, for KSC1 and KSC2 data and models, plotted as days after emergence.

Fig. 5. (a) Biomass B for USU1, USU2, KSC1, and KSC2 data and models. (b) ΔB = modeled B - measured B.

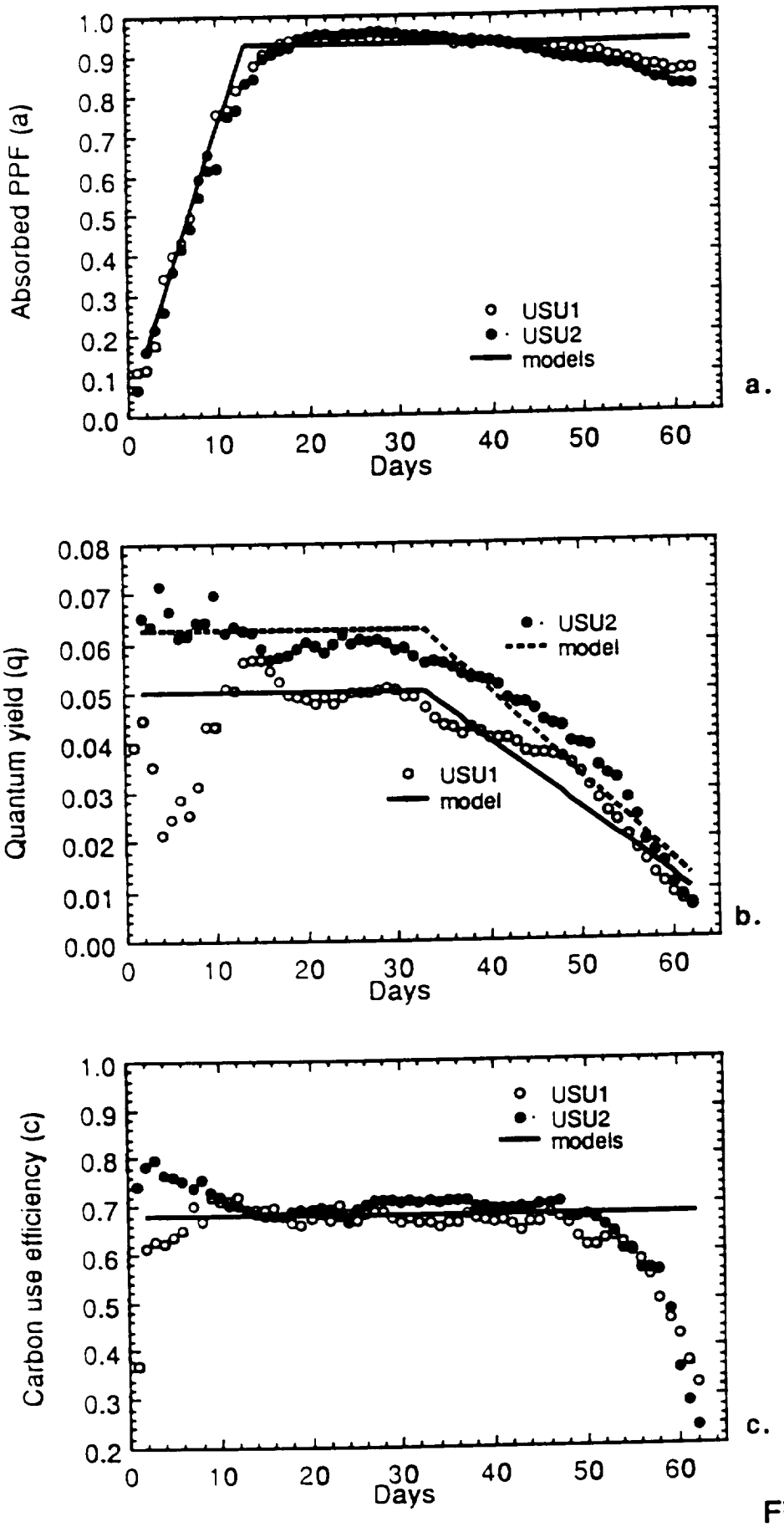
Absorbed PPF (a)
1.0
0.9
0.8
0.7
0.6
0.5
0.4
0.3
0.2
0.1
0.0
0
10
20
30
40
50
60
Days
USU1
USU2
models
a.
Quantum yield (q)
0.08
0.07
0.06
0.05
0.04
0.03
0.02
0.01
0.00
0
10
20
30
40
50
60
Days
USU2
model
USU1
model
b.
Carbon use efficiency (c)
1.0
0.9
0.8
0.7
0.6
0.5
0.4
0.3
0.2
0
10
20
30
40
50
60
Days
USU1
USU2
models
c.

FIG. 1

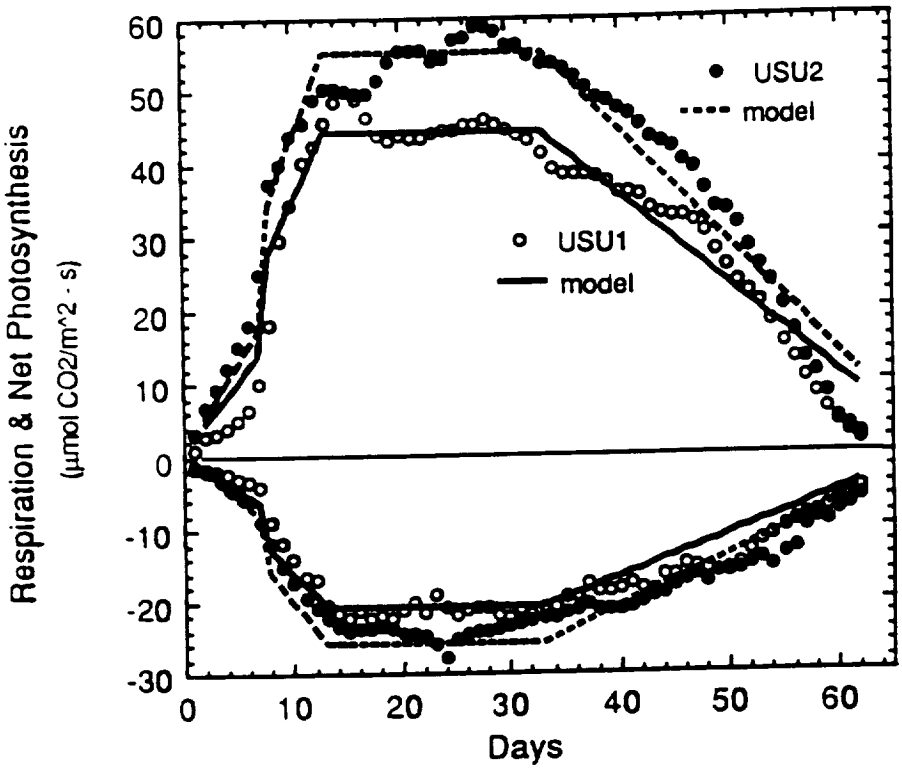
Respiration & Net Photosynthesis
(µmol CO2/m^2 · s)
60
50
40
30
20
10
0
-10
-20
-30
0
10
20
30
40
50
60
Days
USU2
model
USU1
model

a.

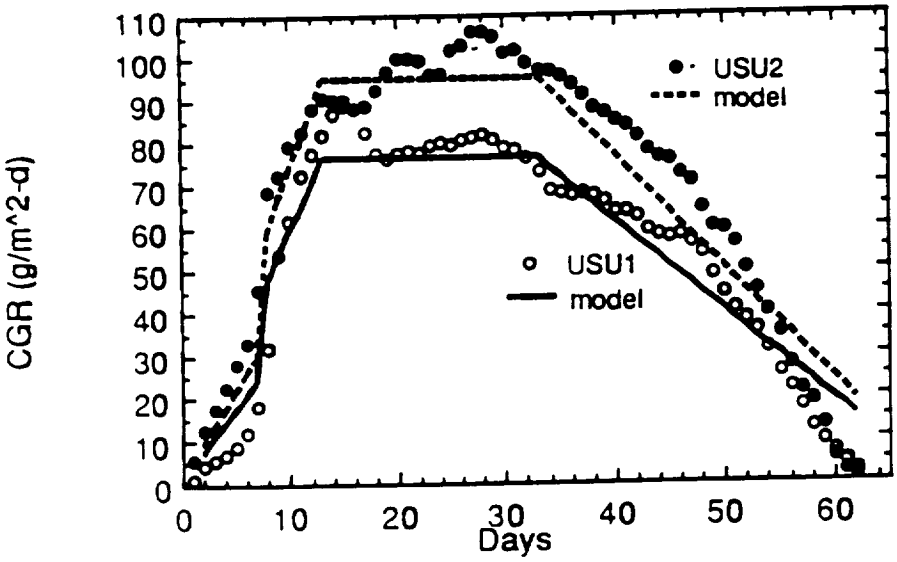
CGR (g/m^2-d)
110
100
90
80
70
60
50
40
30
20
10
0
0
10
20
30
40
50
60
Days
USU2
model
USU1
model

b.

FIG. 2

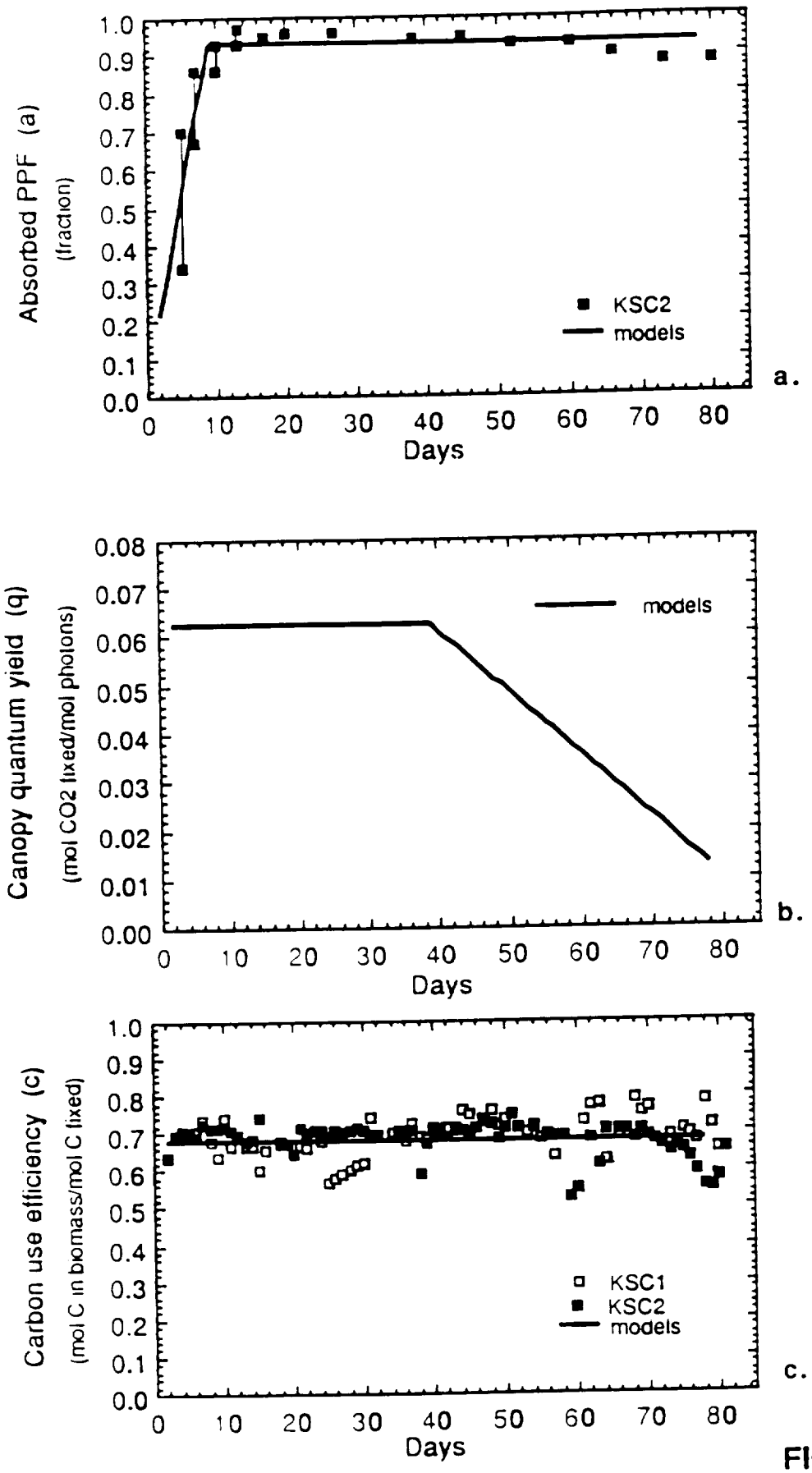
Absorbed PPF (a)
(fraction)
1.0
0.9
0.8
0.7
0.6
0.5
0.4
0.3
0.2
0.1
0.0
0
10
20
30
40
50
60
70
80
Days
KSC2
models
a.
Canopy quantum yield (q)
(mol CO2 fixed/mol photons)
0.08
0.07
0.06
0.05
0.04
0.03
0.02
0.01
0.00
models
b.
Carbon use efficiency (c)
(mol C in biomass/mol C fixed)
KSC1
KSC2
models
c.

FIG. 3

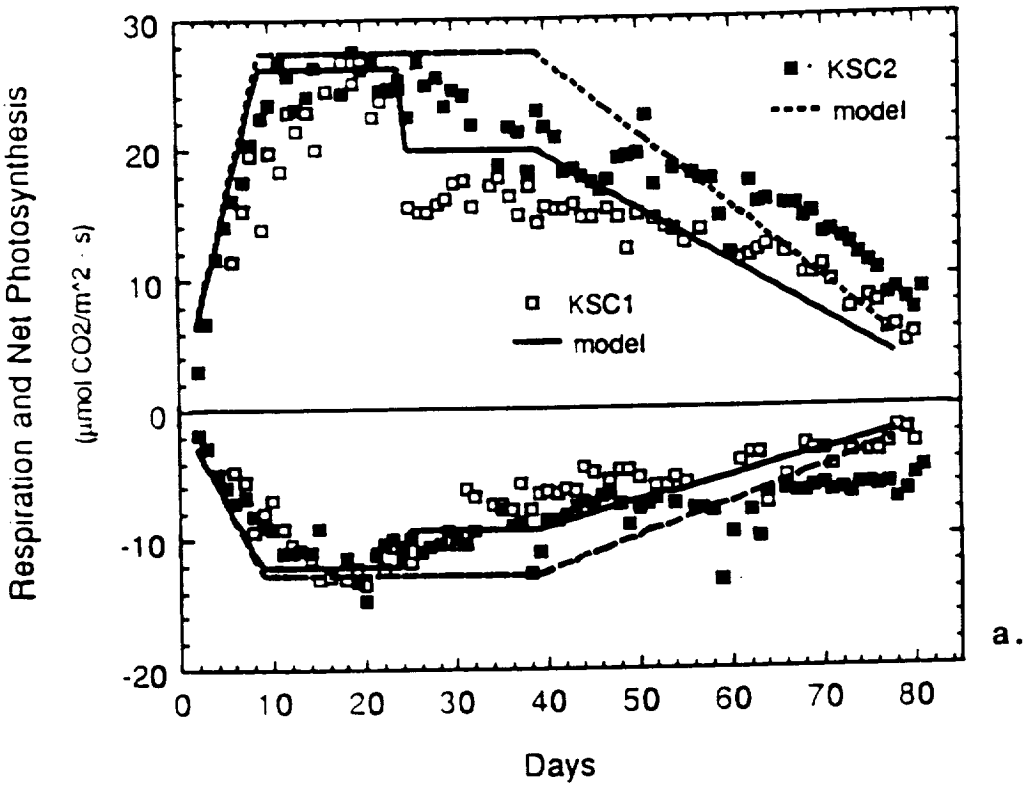
Respiration and Net Photosynthesis
(μmol CO2/m^2 · s)
30
20
10
0
-10
-20
0
10
20
30
40
50
60
70
80
Days
KSC2
model
KSC1
model
a.

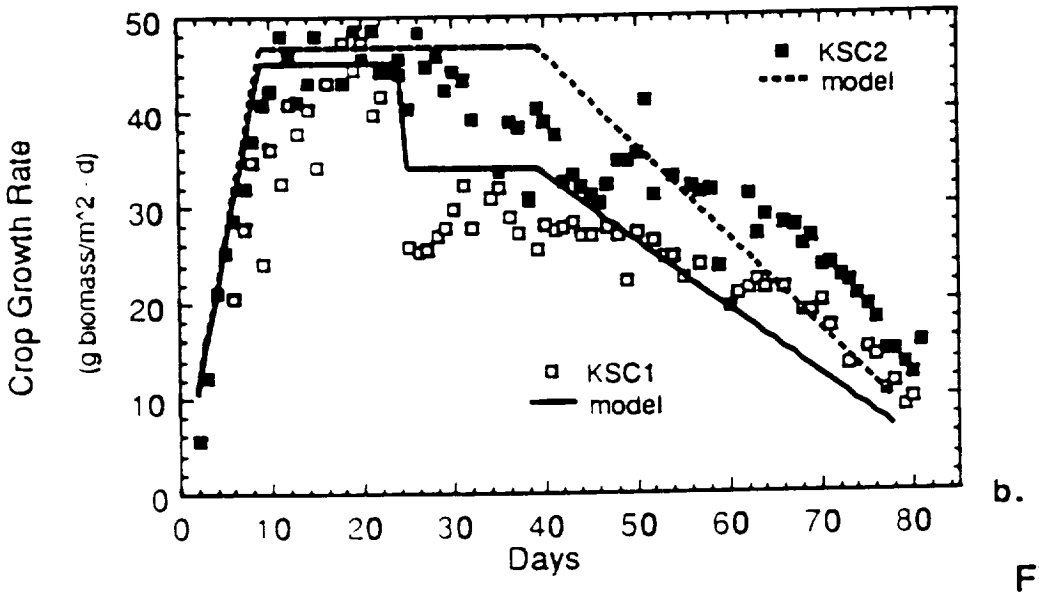
Crop Growth Rate
(g biomass/m^2 · d)
50
40
30
20
10
0
0
10
20
30
40
50
60
70
80
Days
KSC2
model
KSC1
model
b.

FIG. 4

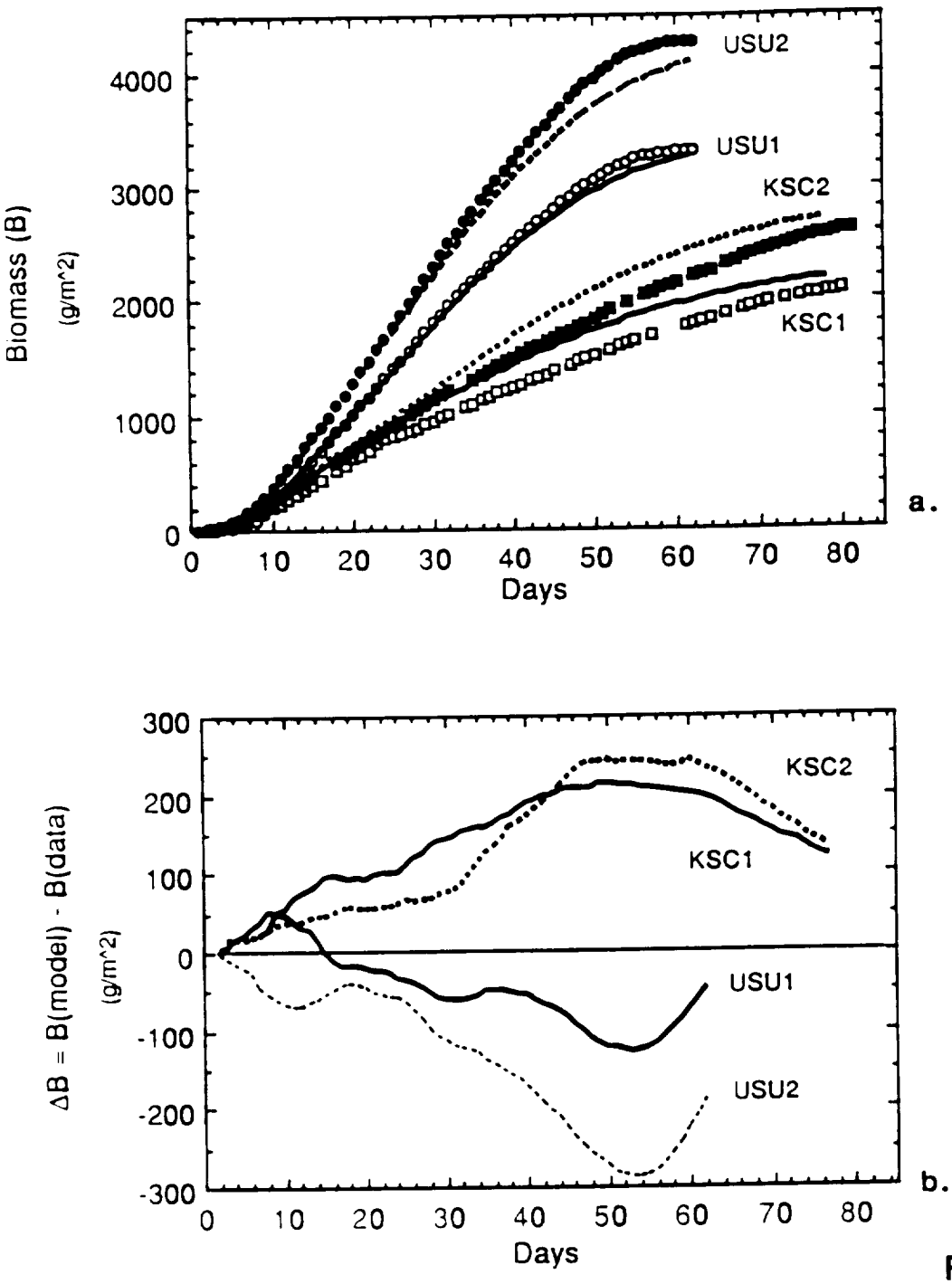
Biomass (B)
(g/m^2)
4000
3000
2000
1000
0
0
10
20
30
40
50
60
70
80
Days
USU2
USU1
KSC2
KSC1
a.
ΔB = B(model) - B(data)
(g/m^2)
300
200
100
0
-100
-200
-300
0
10
20
30
40
50
60
70
80
Days
KSC2
KSC1
USU1
USU2
b.

FIG. 5

Other Accomplishments

In this section I would like to note reprints from the following papers:

Volk, T., and B. Bugbee, Modeling light and temperature effects on leaf emergence in wheat and barley, *Crop Science, 31*, 1218-1224, 1991.

Volk, T., Comments on bioprocessing in space, *Enzyme and Microbial Technology, 15*, 899-900, 1993.

For convenience, these two reprints are at end of this section. This section also includes abstracts and comments on two other papers and a list of papers presented, meetings attended, and collaborative visits to CELSS sites.

Volk, T., Mathematical modeling of CELSS, *Foundations of Space Biology and Medicine*, chapter 15, in press, 1993.
ABSTRACT: Before full CELSS are constructed, mathematical models will be built to explore various aspects of the dynamics of the system, to test the influence of different configurations, the additions of alternative components, the operation during and after various failure modes. Perhaps the most crucial function of the models at this early stage of development is their ability to formalize and communicate the experimental findings from the disciplines dealing with the CELSS components. Findings from disciplinary studies in nutrition, crop growth, engineering, and control theory are linked by the modelers of CELSS.

These subdisciplines of the science of CELSS correspond to the major physical components: the human inhabitants, the crops, and the recycling systems, and the control systems. Each has its own unique challenges involving modeling and will be examined in turn: diet models, crop growth models, engineering models, and models of system dynamics. Finally, we must also ask how these disciplines are pieces in the larger picture.

COMMENTS: I believe that the four "challenges involving modeling" in this overview work can serve as a framework for organizing CELSS modeling efforts.

Volk, T. and H. Cullingford, Crop growth and associated life support for a lunar farm, *The Second Conference on Lunar Bases and Space Activities of the 21st Century*, edited by W. W. Mendell, NASA Publication CP-3166, 705 pp., 525-530, 1992.

ABSTRACT: Supporting human life on a lunar base will require growing many different food crops. This paper investigates the growth dynamics of four crops—wheat, soybeans, potatoes, and lettuce—for general similarities and differences along with associated material flows of the gases, liquids, and solids in a lunar farm. The human dietary requirements are compared with the protein, carbohydrate, and lipid contents of these hydroponically-grown, high productivity crops to derive a lunar farm diet. A simple and generic analytical model is used to calculate the mass fluxes of CO_2, H_2O, HNO_3, and O_2 during the life cycle of each of the four crops. The resulting farm crop areas are given along with the corresponding biomass production rates. One significant conclusion of this study is that there is a "lipid problem" associated with the incorporation of these four crops into a viable diet.

COMMENTS: This paper summarizes a modeling approach followed early during the grant. However, as I discovered and reported in my 1 Dec. 1990 - 31 May 1991 Status Report, this double logistic "early" model must be (and eventually was) superseded. While the double logistic model seemed adequate years ago when CELSS crop data consisted of a few points for biomass as a function of time, it was inadequate to do justice to the more recent an detailed gas exchange data of CO_2 uptake rates during the life cycle. In addition, the double logistic model could not be reconciled with the components of the energy cascade, since it could not adequately use the physiological and energetic components of the gas exchange data. The superseding system is the energy cascade model presented in this report.

Papers presented, meetings attended, and collaborative visits to CELSS sites.

Science and Technology Working Group for NASA Space Station CELSS Test Facility, Los Gatos, CA, 20-22 July, 1993.

CELSS photosynthesis workshop, convened by B. Bugbeee, Utah State University, Logan, UT, 6-9 March, 1993.

Volk, T., Plants in life support: mass and energy fundamentals for models, invited presentation at CELSS '93: Controlled Ecological Life Support Systems PI meeting, Alexandria, VA, 1-4 March, 1993.

Tubiello, F., and T. Volk, A modified version of the Ceres-wheat model to simulate CELSS experiments, poster, CELSS '93: Controlled Ecological Life Support Systems, PI meeting, Alexandria, VA, 1-4 March, 1993.

Science and Technology Working Group for NASA Space Station CELSS Test Facility, Burlingame, CA, 17-19 November, 1992.

American Society of Agronomy, annual meeting, Minneapolis, Minnesota, 1-6 November, 1992.

Volk, T., Impact of crop modeling on CELSS system design, presented at NSCORT seminar, Purdue University, 26 October, 1992. Private meetings with Drs. Nelson, Sherman, Ladisch, Nielson, Hasegawa, and Hodges.

Science and Technology Working Group for NASA Space Station CELSS Test Facility, Carmel, CA, 21-24 July, 1992.

Collaboration at Utah State University with Bruce Bugbee and meeting with CELSS site visit group (Galston committee), April 1992.

Science and Technology Working Group for NASA Space Station CELSS Test Facility, Napa, CA, 25-27 February, 1992.

Science and Technology Working Group for NASA Space Station CELSS Test Facility, Larkspur, CA, 7-10 October, 1992.

Volk, T., A four-component strategy for CELSS models: diet, crop growth, engineering, and systems, invited presentation at the NASA Workshop on Life Support Systems Analysis, Milwaukee, WI, 25-27 June, 1991.

Collaboration with Ray Wheeler and Wade Berry at Kennedy Space Center, June 1991.

Collaboration with Robert MacElroy, Charles Blackwell, and David Bubenheim at Ames Research Center, June 1991.

The Optimization of Plant Productivity, NASA/USDA Int. Conf., Cocoa Beach, Florida, March 7-9, 1991.

Volk, T., Issues in modeling bioregenerative life support systems, invited presentation at Joint Soviet-American Symposium on Artificial Biospheres, Krasnoyarsk, U.S.S.R., April 23-27, 1990.

Collaboration with Bruce Bugbee at Utah State University, August 1989.

Collaboration with David Raper at North Carolina State University, April 1989.

Modeling Light and Temperature Effects on Leaf Emergence in Wheat and Barley

Tyler Volk* and Bruce Bugbee

ABSTRACT

Phenological development affects canopy structure, radiation interception, and dry matter production; most crop simulation models therefore incorporate leaf emergence rate as a basic parameter. A recent study examined leaf emergence rate as a function of temperature and daylength among wheat (*Triticum aestivum* L.) and barley (*Hordeum vulgare* L.) cultivars. Leaf emergence rate and phyllochron were modeled as functions of temperature alone, daylength alone, and the interaction between temperature and daylength. The resulting equations contained an unwieldy number of constants. Here we simplify by reducing the constants by >70%, and show leaf emergence rate as a single response surface with temperature and daylength. In addition, we incorporate the effect of photosynthetic photon flux into the model. Generic fits for wheat and barley show cultivar differences less than ±5% for wheat and less than ±10% for barley. Barley is more sensitive to daylength changes than wheat for common environmental values of daylength, which may be related to the difference in sensitivity to daylength between spring and winter cultivars. Differences in leaf emergence rate between cultivars can be incorporated into the model by means of a single, nondimensional factor for each cultivar.

In a series of three papers (Cao and Moss, 1989a,b,c; hereafter C&M-a, C&M-b, and C&M-c), Cao and Moss computed the leaf emergence rate (LER, leaves d^{-1}) for wheat and barley by counting the number of leaves on the main stem as a function of time. The slope of leaves vs. time was used to estimate the emergence rate. They found a linear relationship; i.e., LER is constant for a given environment from the time of seedling emergence and up to 20 d, or approximately the third leaf. They also were concerned with a related quantity, the phyllochron (P in degree-days $leaf^{-1}$), which is the thermal time required for the emergence of each leaf. As they stated, these quantities are important in many dynamic simulation models and need refinement.

They conducted experiments using four soft-white winter wheat cultivars and four spring barley genotypes. Temperature and daylight hours were varied to determine the effect on LER and P. Temperature (T) varied from 7.5 to 25 °C. Daylight hours (D), with a photosynthetic photon flux density of 400 $\mu mol\ m^{-2}\ s^{-1}$, varied from 6 to 24 h.

Cao and Moss fit curves for LER and P as functions of T (C&M-a), as functions of D (C&M-b), and as functions of a synthetic quantity they called the thermal-photo ratio, TD^{-1}, in degree-days per hour (C&M-c). Their equations are useful, but have important inconsistencies. Our objective was to combine their findings into a single equation for LER that will simplify the application in larger models. For symbols and variables used, see Table 1.

T. Volk, Dep. of Applied Science, 26 Stuyvesant St., New York Univ., New York, NY 10003; and B. Bugbee, Plants, Soils, and Biometeorology Dep., Utah State Univ., Logan, UT 84322-4820. Support provided by NASA Cooperative Agreements NCC2-608 (for T. Volk) and NCC2-139 (for B. Bugbee). Received 31 May 1990. *Corresponding author.

Published in Crop Sci. 31:1218–1224 (1991).

RESULTS FROM CAO AND MOSS

Temperature Effects

The results of an experiment to isolate temperature effects were reported in C&M-a. With D = 14 h, T was varied between 7.5 and 25 °C at intervals of 2.5 °C. Data points for LER and P fell along smooth curves. They fit LER and P with the following equations:

$$LER = c_1 + c_2T - c_3T^2 \quad [1a]$$

$$P = c_4 \exp(c_5T) \quad [1b]$$

The constants, c_1 to c_5, were fit for each of the eight cultivars of wheat and barley.

Daylength Effects

Photoperiod effects were examined in C&M-b. With T = 15 °C, D was varied at 8, 10, 12, 14, 16, 18, 21, and 24 h. As with the T variation, the resulting LER and P were smooth curves. They fit these data with the following equations:

$$LER = \frac{D}{c_6 + c_7D} \quad [1c]$$

$$P = \frac{c_8 + c_9D}{D} \quad [1d]$$

These equations require four new constants. Note that $c_6 \neq c_8$ and $c_7 \neq c_9$, because, as explained more fully below, P and LER vary by a factor that must include T.

Temperature and Daylength Interactions

In C&M-c, Cao and Moss examined the value for the phyllochron in experiments in which T = 10, 15, and 20 °C, and D = 6, 10, 14, and 18 h. When these 12 points were plotted against a thermo-photo ratio, a term proposed by Cao and Moss with the units of degree-days per hour of photoperiod (TD^{-1}), there was a linear correlation. The following equation was used to fit this data:

$$P = c_{10} + c_{11}\frac{T}{D} \quad [1e]$$

Since C&M-c emphasized the phyllochron, the data and potential models for LER were not shown.

Choices among Models

There are several inconsistencies in the results reported by Cao and Moss. For example, consider Eq. [1a] and [1b]. Presumably, a modeler could select either Eq. [1a] for LER or Eq. [1b] for P, depending on the needs of the model. However, P is usually defined as a function of LER, T, and a constant base temperature (T_b):

$$P = \frac{T - T_b}{LER} \quad [2]$$

Abbreviations: LER, leaf emergence rate; PPF, photosynthetic photon flux. See also Table 1.

Table 1. List of symbols used in modeling light and temperature effects on leaf emergence in wheat and barley.

Symbol	Name	Units
D	daylength, photoperiod	h
T	temperature	°C
LER	leaf emergence rate	leaves d^{-1}
P	phyllochron	degree-days $leaf^{-1}$
PPF	photosynthetic photon flux	mol m^{-2} d^{-1}
PPF_0	value for PPF where LER = 0	mol m^{-2} d^{-1}
PPF_{hf}	PPF half-saturation constant	mol m^{-2} d^{-1}
c_i	constants in Eq. [1a–e]	various dimensions
D_{hf}	photoperiod half-saturation constant	h
T_{max}	temperature at maximum LER	°C
a_i	constants in Eq. [3a]	various dimensions
a	rate constant in Eq. [3b]	leaves d^{-1}
b	maximum LER in Eq. [3c]	leaves d^{-1}
d	maximum LER in Eq. [5a]	leaves d^{-1}
r	rate constant in improved model, Eq. [4]	leaves d^{-1}
f	factor to account for PPF effect on LER	nondimensional

Using this definition, a modeler could select either Eq. [1a] or Eq. [1b] and calculate both LER and P. Note that Eq. [1a] and [1b], taken as a pair, do not satisfy the relation of definition between P and LER in Eq. [2], and therefore present an inconsistency.

A similar choice confronts the modeler computing LER and P for a specified daylength. Again, two equations, Eq. [1c] and [1d], functionally could be reduced to one by using the definition in Eq. [2].

Most growth models require knowledge of LER as a function of both T and D. C&M-c presents a potential solution to the interaction between T and D in Eq. [1e]; however, a model for the interaction of T and D should indicate how T varies with constant D and how D varies with constant T. If so, then Eq. [1e] with D equal to a constant should be identical (in the structure of its variables and constants) to Eq. [1b]. This is not the case here: Eq. [1e] with D equal to a constant shows P to be a linear function of T, while in Eq. [1b] P varies exponentially with T. The different solutions shown by Cao and Moss present difficulties for the modeler who must select, perhaps arbitrarily, from among several possibilities.

THE IMPROVED MODEL

Temperature and Daylength Effects

It appears that smooth curves for LER and P as a function of D in Eq. [1c] and [1d] could alternatively have been fit with either parabolic or exponential curves, like those used in Eq. [1a] and [1b]. Cao and Moss did not explain why they chose their functions.

We develop a single model that is simple and physiologically meaningful. First, we suggest deriving an equation either for LER or for P, and then consistently calculating the other, if required, using Eq. [2]. We select LER as the fundamental property of the plant, because it is a rate. Also, the phyllochron definition is not universal; it can also be defined as days per leaf.

For the effect of temperature alone we select a parabolic form. A parabola accounts for both positive and negative effects of T on LER. When T is close to the baseline temperature, an increase in T increases development, which increases LER. As T becomes large, negative effects begin to dominate; e.g., protein denaturation rates increase with temperature (Morowitz, 1975), which slows the development. This is similar to the idea behind the logistic equation (see Causton and Venus, 1981, for a review of its applications), with a positive first-order term and a negative second-order term.

A parabola was one form used in C&M-a; see Eq. [1a]. We eliminate the additive constant c_1 for the following reasons. Since the data for wheat and barley (C&M-a) showed a base temperature of 0.02 °C, Cao and Moss used 0 °C as the base temperature to compute the degree-days for P; in other words, $T_b = 0$ °C in Eq. [2]. For consistency, this demands that $c_1 = 0$ in Eq. [1a]. Therefore, an equation for LER as a function of T alone is:

$$\text{at constant } D,\ \text{LER} = a_1 T - a_2 T^2 \qquad [3a]$$

Eq. [3a] describes a parabolic curve where $\partial \text{LER}/\partial T = 0$ at $T = T_{max}$. T_{max} is a useful concept—for example, Cao and Moss compared T_{max} across cultivars—and we use it to recast Eq. [3a]:

$$\text{at constant } D,\ \text{LER} = a\left[\frac{T}{T_{max}}\left(2 - \frac{T}{T_{max}}\right)\right] \qquad [3b]$$

In Eq. [3b] there are still two fitting parameters, a and T_{max}. The term inside the square brackets equals 1 when $T = T_{max}$, and thus a is the maximum leaf emergence rate.

Our equation for photoperiod dynamics is similar to Eq. [1c], but is expressed in the more traditional form of the Michaelis–Menton equation:

$$\text{at constant } T,\ \text{LER} = \frac{b\,D}{D_{hf} + D} \qquad [3c]$$

Eq. [3c] has two fitting parameters, b and D_{hf}. The term b is the maximum development rate, for as D becomes large, LER approaches the value of b. In our case, D is constrained to a maximum of 24 h, and thus the actual maximum value of LER may be significantly less than the mathematical maximum b. The term D_{hf} is the half-saturation constant, and when $D = D_{hf}$, LER is exactly half of its maximum value b. This equation is commonly used in growth dynamics, where growth increases as a function of some parameter, then levels off to an asymptotic maximum.

Response Surface with Temperature and Daylength

The LER is a function of T at constant D in Eq. [3b] and a function of D at constant T in Eq. [3c]. Equations [3b] and [3c] should be the functional forms for LER that can be derived from a response surface for LER, where the dependent LER results from independent variation of both T and D. This is possible by forming a surface from the product of the right sides of Eq. [3b] and [3c]. Performing this multiplication, and letting $r = ab$, we obtain:

$$\text{LER} = r\left[\frac{T}{T_{max}}\left(2 - \frac{T}{T_{max}}\right)\right]\left[\frac{D}{D_{hf} + D}\right] \qquad [4]$$

In Eq. [4], both terms in brackets are nondimensional and therefore r has the same units as LER, or leaves per day. This is a simple system: a rate is multiplied by two nondimensional terms that are functions of only T and only D, respectively. There are only three free parameters, compared to eleven in Eq. [1a–1e]. Furthermore, the three free parameters (r, T_{max}, and D_{hf}) are relevant to plant growth: a rate, an optimal temperature, and a photoperiod. Computing the phyllochron does not add any additional parameters, because P can be computed from its definition in Eq. [2].

Daily Photosynthetic Photon Flux in the Response Surface

Temperature and photoperiod are the dominant factors influencing LER, but the total daily PPF can be important at low light levels, when there is insufficient photosynthate for normal cell division and expansion, or when comparing equal day lengths with instantaneously varying values of flux density. Friend et al. (1962) found that LER decreased by 30% as PPF was decreased from 43 mol m^{-2} d^{-1} (typical summer daily integral) to 3 mol m^{-2} d^{-1} (near the light compensation point), and this result was recently confirmed by Barnes and Bugbee (1991) (Fig. 1). Bugbee and Salisbury (1988) examined the effect of high PPF levels on development rate and found that days to anthesis (a sensitive indicator of developmental rate) was not affected by 23 to 92 mol m^{-2} d^{-1}. This finding is not consistent with Friend et al., who found that LER continued to increase from 30 to 43 mol m^{-2} d^{-1}. Some of the effect of PPF on LER in the Friend et al. study may have been due to temperature. Rickman et al. (1985) found that the temperature of the stem base (leaf growing point) increased with increasing PPF, and that almost all of the effect of PPF on LER was explained by the temperature change. It is extremely difficult to maintain a constant plant temperature with increasing radiation unless chilled water baths are installed below the lamps. Water baths were used by both Barnes and Bugbee (1991) and Bugbee and Salisbury (1988), but not by Friend et al. (1962). The effect of PPF is probably negligible above 30 mol m^{-2} d^{-1} and this parameter could therefore be ignored in most field studies.

The effects of PPF cannot be ignored, however, in studies below 30 mol m^{-2} d^{-1}, which is the case for some of the Cao and Moss values. We account for the effects of PPF on leaf emergence rate by specifying the following conditions: (i) a minimum value of PPF required to balance maintenance respiration (PPF_o); (ii) a positive correlation between PPF and LER at relatively low levels of PPF; and (iii) relatively little effect of PPF due to saturation at increasingly higher levels of PPF. These conditions can be satisfied by a modified Michaelis–Menton equation, and we write:

at constant T and D,

$$LER = d\frac{PPF - PPF_o}{(PPF_{hf} - PPF_o) + (PPF - PPF_o)} \quad [5a]$$

In Eq. [5a], two constants, PPF_{hf} and PPF_o, are introduced, and the difference $PPF_{hf} - PPF_o$ is similar in meaning to D_{hf} in Eq. [3c]. The overall shape of the

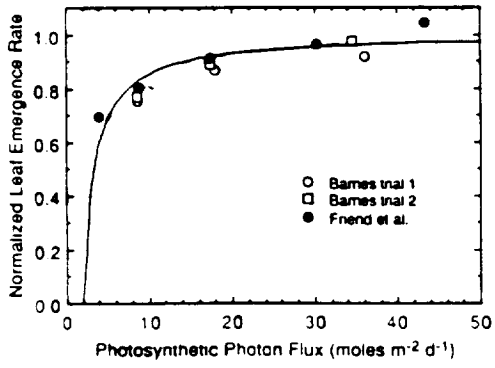

Fig. 1. Fit to data of Barnes and Bugbee (1991) and Friend et al. (1962) using Eq. [5a] with d = 1. Data have been normalized and combined using procedure described in text, and assuming minimal photosynthetic photon flux required to balance maintenance respiration (PPF_o) = 2 mol m^{-2} d^{-1}. Best fit yields half-saturation PPF_{hf} = 3.4 mol m^{-2} d^{-1}.

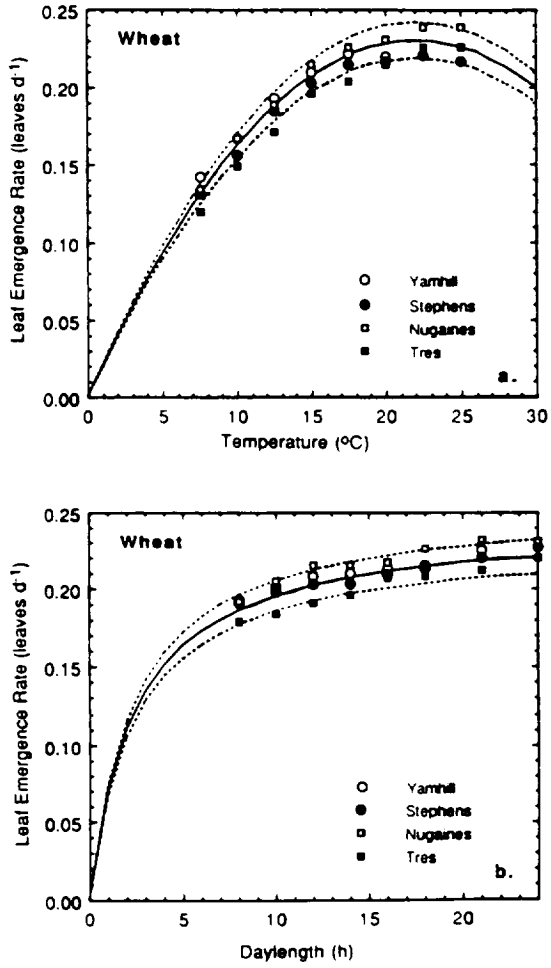

Fig. 2. Model curves generated from Eq. [4] at various conditions of (a) constant daylength D = 14 h and (b) constant temperature T = 15 °C for comparison with data for wheat genotypes from Cao and Moss (1989a,b). Model plots (solid lines) use rate r = 0.27 leaves d^{-1}, half-saturation daylength D_{hf} = 2.4 h, T_{max} = 22 °C. Effect of increasing and decreasing r by 5% shown by dotted lines. Cao and Moss data has been corrected for PPF using Eq. [5b] and Fig. 1, as described in the text.

function derives from the differences between the terms PPF and PPF_o and between PPF_{hf} and PPF_o. The constant d is a rate with the same units as LER.

It is possible to incorporate the effect of PPF on LER by multiplying the right hand side of Eq. [4] by the right hand side of Eq. [5a] and eliminate d by subsuming it in the term r. This would add two additional constants to the response surface, making a total of five. However, because PPF is important only in low light, we propose using the inverse of Eq. [5a] to adjust LER so that the effect of PPF can be eliminated before using Eq. [4].

We define a coefficient (f) that can be used to adjust the data for LER from Cao and Moss to eliminate the effect of PPF, as follows:

$$f = \frac{(PPF_{hf} - PPF_o) + (PPF - PPF_o)}{PPF - PPF_o} \quad [5b]$$

The function f is computed using data from Barnes and Bugbee (1991) and Friend et al. (1962) using a two-step fitting procedure. First, we separately fit the two data sets using Eq. [5a] to derive a different PPF_{hf} and d for each. Each value for LER from the two data sets is then normalized by dividing by the respective fitted ds, which allows the two sets of data to be combined into a single, normalized set (Fig. 1). Finally, this combined set is fit to derive a single value of PPF_{hf}. In the normalized combined set, d is equal to unity. We assume PPF_o = 2 mol m^{-2} d^{-1}. Changing this across a reasonable range (0–5 mol m^{-2} d^{-1}) of values produces only small effects (≈1%) on the calculated correction factors.

With PPF_o and the fitted PPF_{hf}, Eq. [5b] is used to multiply each value for LER in the Cao and Moss data set by f. Lacking additional data, we assume that LER for barley can be modified to remove the effect of PPF by the same function that we have derived for wheat. For Cao and Moss's lowest values of PPF (8 h light at 400 μmol m^{-2} s^{-1}, or ≈11.5 mol m^{-2} d^{-1}), f is ≈1.15. With 24 h of daylength, f is ≈1.04 in the Cao and Moss experiments. The lower end of PPF in the Bugbee and Salisbury (1988) experiments is approximately the higher end of PPF in the Cao and Moss experiments; Bugbee and Salisbury thus noted no significant effect because the effect of PPF was close to saturation.

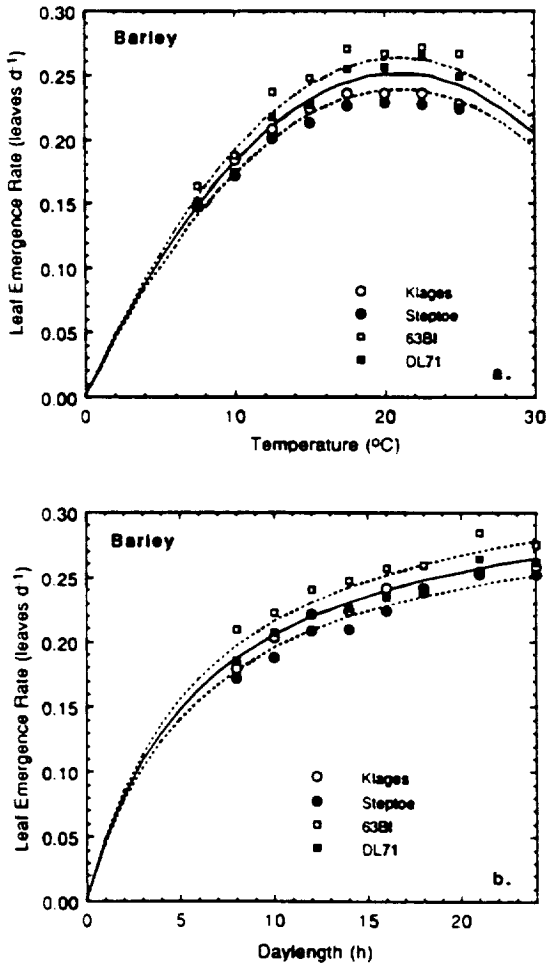

Fig. 3. Model curves generated from Eq. [4] at various conditions of (a) constant daylength D = 14 h and (b) constant temperature T = 15 °C for comparison with data for barley genotypes from Cao and Moss (1989a,b). Model plots shown use rate r = 0.36 leaves d^{-1}, half-saturation daylength D_{hf} = 6.3 h, T_{max} = 21 °C. Effect of increasing and decreasing r by 5% shown by dotted lines. Cao and Moss data has been corrected for PPF using Eq. [5b] and Fig. 1, as described in the text.

Response Surface Compared to Data

The data of Cao and Moss were fit using Eq. [4], after modification for the effect of PPF as just explained. If either D or T are assumed to be constant, then Eq. [4] is equivalent to two of Cao and Moss's original equations (here, Eqs. [1a] and [1c], with c_1 = 0 in Eq. [1a]). Cao and Moss proved that such formulations will fit the data for individual cultivars with a high correlation coefficient ($r^2 > 0.97$ in all cases, and usually > 0.99).

Comparisons among the wheat cultivars considered as a group, and among the barley cultivars considered as a group, could emphasize either the differences or the similarities. To examine these issues, we have combined into groups the four cultivars of wheat and the four of barley for fitting with our model.

The results for wheat and barley are shown in Fig. 2 and 3, respectively. Model fits using Eq. [4] are dis-

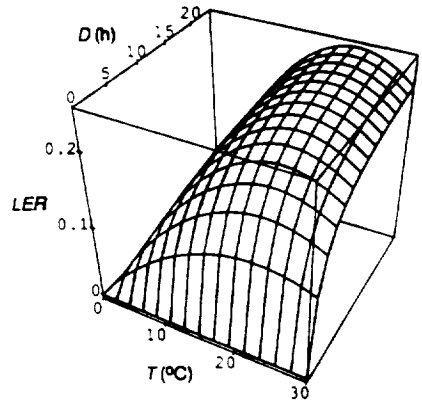

Fig. 4. Three-dimensional response surface for wheat LER (leaf emergence rate) as a function of T and D, using Eq. [4] with the constants identical to those in Fig. 2 (rate r = 0.27 leaves d^{-1}, T_{max} = 22 °C, and half-saturation daylength D_{hf} = 2.4 h).

played for the two two-dimensional sections where the most data were taken by Cao and Moss, varying T at constant D = 14 h and varying D at constant T = 15 °C.

For a conceptual picture of the response surface, LER for wheat as a function of T and D in three dimensions is shown in Fig. 4. For a numerical picture of the response surface, contour plots of LER for wheat and barley as a function of T and D are shown in Fig. 5. It is evident from the contour plots that LER has little sensitivity to D at low values of T and little sensitivity to T at low values of D. Low values of either environmental factor limit the potential variation in LER due to the other factor.

Our model provides a unified interpretation of the forcing processes. In contrast, the thermo-photo ratio sometimes used (C&M-c being one example) needs to be critically examined. Our model in Eq. [4] is not equivalent to Eq. [1e]. When the systems of Eq. [2] and [4] are used to plot P vs. TD^{-1} (for comparison with the analogous plot in C&M-c) the generated points are scattered across a field, rather than along a single line. In contrast, with our model, temperature, photoperiod, and leaf emergence rate can be expressed as a parsimonious three-dimensional response surface, as shown in Fig. 4. The thermo-photo ratio does not represent the behavior of the system, and we recommend Eq. [4] as the model for the interaction of T and D.

Figures 2 and 3 exhibit differences among cultivars. In our opinion, these differences are relatively small; the wheat cultivars fall within ≈5% of the group fit; the corresponding value for barley is somewhat larger, ≤10%. These data should be weighed into the modeling objectives to determine the utility of working toward separate coefficients for each cultivar against the streamlining possible with a single generic set of coefficients that could apply to all cultivars.

There are strong similarities in shapes among the grouped cultivars. Specifically, Fig. 2 and 3 show that usually the LER for any particular cultivar is consistently above or below the generic fit. This observation can be incorporated easily into the model by modifying the rate multiplier r in Eq. [4] by a nondimensional cultivar factor. Table 2 lists the cultivar factors which give the least-squares fits for the wheat and barley cultivars. They range from 0.97 to 1.04 for the

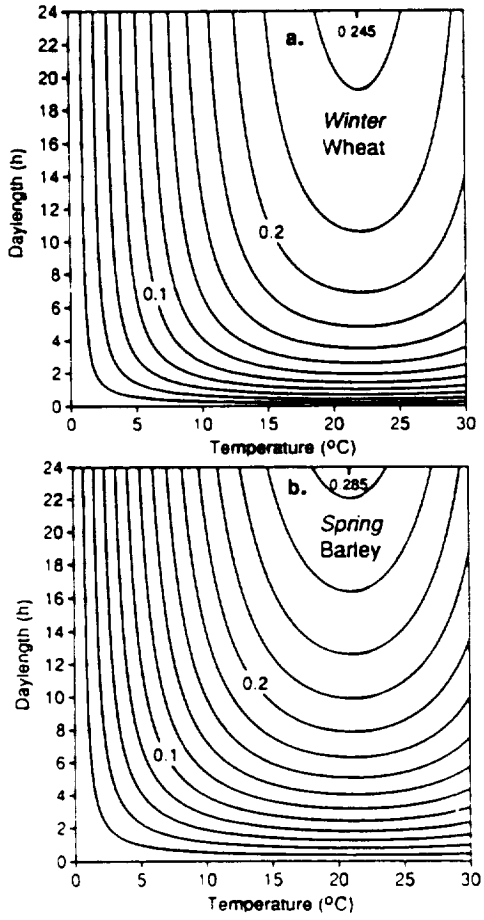

Fig. 5. Contour plots of the response surface for LER (leaf emergence rate) as a function of temperature T and daylength D. (a) Wheat. Constants identical to those in Fig. 2 (rate r = 0.27 levels d^{-1}, T_{max} = 22 °C, and half-saturation daylength D_{hf} = 2.4 h). (b) Barley. Constants identical to those in Fig. 3 (r = 0.36 leaves d^{-1}, T_{max} = 21 °C, and D_{hf} = 6.3 h).

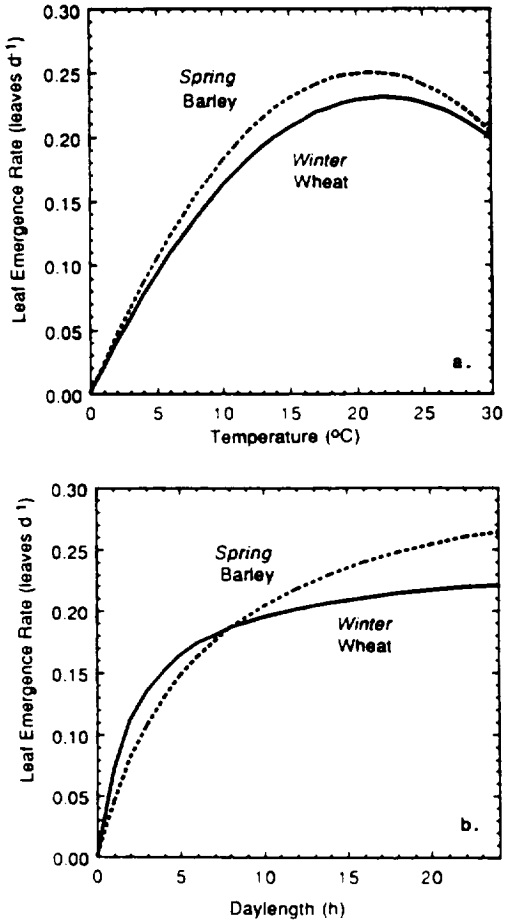

Fig. 6. The fits from Fig. 2 and 3 combined to compare and contrast wheat and barley. (a) The temperature curves are for daylengths of 14 h. (b) The daylength curves are for temperatures of 15 °C. Since all wheat cultivars are winter and all barley cultivars are spring, similarities in temperature response and differences in daylength response may be due to behaviors inherent in spring and winter cultivars.

wheat cultivars, and from 0.94 to 1.08 for the barley cultivars. The importance of small cultivar differences should not be ignored, because seemingly minor changes during early growth can have important effects on yield. We therefore suggest applying cultivar factors when necessary, and furthermore that the values for T_{max} and D_{hf} listed in Fig. 2 and 3 for wheat (T_{max} = 22 °C, D_{hf} = 2.4 h) and barley (T_{max} = 21 °C, D_{hf} = 6.3 h), may be considered as species properties. In our analysis, the variation among cultivars then occurs among the rates but not the shapes.

In this context, it is useful to compare the average fit to the wheat cultivars with the average fit to the barley cultivars (Fig. 6). We see that because the difference in the value of T_{max} between wheat and barley is so small, the difference in LER between any particular wheat and barley cultivar remains nearly a constant fraction as temperature is varied.

When daylength is varied, a substantial difference in shape occurs between wheat and barley (Fig. 6). Compared to barley, wheat saturates at very low daylengths. The barley cultivars are more sensitive to daylength than the wheat cultivars. In this study, all the barley cultivars were spring and the wheat cultivars winter. The difference in photoperiod sensitivity may be because of inherent differences between wheat and barley, or it may be an inherent difference between spring and winter cultivars.

Both spring and winter cultivars would be planted at about the same photoperiod (12 h; spring or fall equinox, respectively), but 30 d after planting, the daylength would be 3 or 4 h longer in the spring than in the fall (depending on latitude). It may be advantageous for spring cultivars to be more sensitive to daylength than winter cultivars. If spring planting were delayed, it would be useful to have a cultivar that develops rapidly, so that anthesis occurs before the onset of high temperatures. Conversely, if spring planting was early, the LER of the main culm should be slow, to maximize tillering and yield potential.

CONCLUSIONS

This paper presents a model for LER in wheat and barley that is simple and represents temperature and daylength responses. Many questions remain. This model is based on data from constant day–night temperatures. Night temperatures are almost always lower than day temperatures in a natural environment. It may not be appropriate to use an average daily temperature in this model, because temperature responses are typically parabolic and the leaf emergence rate at a constant daily temperature might not be the same as the average leaf emergence rate with diurnal fluctuations in temperature (Erwin and Heins, 1990). In some crops, however, diurnal temperature fluctuations do not affect development rate (Yourstone and Wallace, 1990).

Bauer et al. (1984) found that N and water supply did not alter the rate of wheat development of the main stem within certain bounds. Longnecker et al. (1990), however, found that N deficiency reduced LER. The effect of N on LER may be similar to that of PPF; development is somewhat affected only after growth is severely reduced. Other factors that have large effects on growth have the potential to alter development. The two variables in this study (temperature and photoperiod) almost completely control the rate of development in wheat (Bauer et al., 1984), but leaf area and yield are affected by many other variables. One could also quantify possible differences between wheat and barley in their response to changing PPF.

Table 2. Factors for modification of r in Eq. [4] to fit individual cultivars (Fig. 2 and 3).

Cultivar	Cultivar factor
Wheat	
Yamhill	1.01
Stephens	0.99
Nugaines	1.04
Tres	0.97
Barley	
Klages	0.98
Steptoe	0.94
63BI	1.08
DL97	1.01

Our model is based on data from plants in early vegetative growth stages. Temperature and photoperiod also seem to control developmental rate during reproductive development in wheat (Porter, 1984). Photoperiod is less important than temperature in determining the length of the grain-fill period, so perhaps the photoperiod half-saturation constant (D_{hf}) shifts. The general structure of this model may be applicable to other growth stages of small grains, but with appropriate changes for T_{max} and D_{hf} to these other stages. During seed fill, for example, D_{hf} may shift to very low values, nearly eliminating the photoperiod contribution to grain fill.

Other environmental parameters may be useful in refining the model. For example, the temperature at the stem base (≈1–2 cm below the soil surface) should be more useful in predicting LER than air temperature (Rickman et al., 1985). Although there are statistically significant differences among cultivars, refining experimental data and the model for separate cultivars may not be necessary. When such refinement is desired, we recommend multiplying the generic leaf emergence rate by a single cultivar factor, as shown in Table 2.

ACKNOWLEDGMENTS

We thank our reviewers for the succinct questions and comments that prompted us to examine the effect of photosynthetic photon flux and improve the paper, and thank Dwight Fisher for his careful and helpful editing efforts.

REFERENCES

Barnes, C.B., and B.G. Bugbee. 1991. Morphological responses of wheat to changes in phytochrome photoequilibria. Plant Physiol. (In press).

Bauer, A., A.B. Frank, and A.L. Black. 1984. Estimation of spring wheat leaf growth rates and anthesis from air temperature. Agron. J. 76:829–835.

Bugbee, B.G., and F.B. Salisbury. 1988. Exploring the limits of crop productivity: I. Photosynthetic efficiency of wheat in high irradiance environments. Plant Physiol. 88:869–878.

Cao, W., and D.N. Moss. 1989a. Temperature effect on leaf emergence and phyllochron in wheat and barley. Crop Sci. 29:1018–1021.

Cao, W., and D.N. Moss. 1989b. Daylength effect on leaf emergence

and phyllochron in wheat and barley. Crop Sci. 29:1021–1025.
Cao, W., and D.N. Moss. 1989c. Temperature and daylength interaction on phyllochron in wheat and barley. Crop Sci. 29:1046–1048.
Causton, D.R., and J.C. Venus. 1981. The biometry of plant growth. Edward Arnold, London.
Erwin, J.E., and R.D. Heins. 1990. Temperature effects in lily development rate and morphology from the visible bud stage until anthesis. J. Am. Soc. Hortic. Sci. 115:644–646.
Friend, D.J.C., V.A. Helson, and J.E. Fisher. 1962. Leaf growth in marquis wheat, as regulated by temperature, light intensity, and daylength. Can. J. Bot. 40:1299–1311.
Longnecker, N., E.M.J. Kirby, and A.D. Robson. 1990. Genotypic differences in wheat in the increased phyllochron in response to nitrogen deficiency. p. 124. *In* Agronomy abstracts. ASA, Madison, WI.
Morowitz, H.J. 1979. Energy flow in biology. Oxbow, Woodbridge, CT.
Porter, J.R. 1984. A model of canopy development in winter wheat. J. Agric. Sci. 102:383–392.
Rickman, R.W., B. Klepper, and C.M. Peterson. 1985. Wheat seedling growth and developmental response to incident photosynthetically active radiation. Agron. J. 77:283–287.
Yourstone, K.S., and D.H. Wallace. 1990. Effects of photoperiod and temperature on rate of node development in indeterminate bean. J. Am. Soc. Hortic. Sci. 115:824–828.

literature survey

Comments on "Bioprocessing in space"

Tyler Volk

Department of Applied Science, New York University, New York, NY

An analysis developed by Westgate et al. *for the digestible energy of edible and inedible biomass, including hydrolysis and fermentation, is reexamined with state-of-the-art values for the harvest index of hydroponic crops.*

Keywords: Bioprocessing; digestible energy; hydrolysis; fermentation; hydroponic crops; space; harvest index

Westgate *et al.*[1] formalized an important consideration for the design of a Controlled Ecological Life Support System (CELSS) for space exploration and habitation. Namely, since a portion of a crop is inedible, savings can be derived from bioprocessing this otherwise inedible portion into additional food. In their example, bioprocessing reduced the crop growth area from 49 m^2/person-day to 33 m^2/person-day. This comment focuses on the role of the harvest index for these savings.

Harvest index is the ratio of edible to total biomass at crop maturity. For their example, Westgate *et al.* took a value for the harvest index of hydroponic wheat of $h = 0.2$, derived from hydroponic wheat experiments in which the harvest index failed to reach typical field values. However, as they noted, "If the relatively low edible fraction of the fast-growing hydroponic plants is increased, the amount of biomass requiring bioregenerative processing will be reduced." Subsequent experiments by the wheat investigators have succeeded in raising the harvest index of hydroponic wheat under high light conditions to about 0.45.[2] This number has also been achieved under optimal CO_2 by hydroponic soybeans.[3] Another important candidate crop for CELSS is potatoes, which have been grown hydroponically with a harvest index of 0.8.[4] Given the variety of values for the harvest index, and the analytical framework for bioprocessing spearheaded by Westgate *et al.*, it is valuable to generalize this framework as a potential design element for CELSS.

Westgate *et al.* established the dietary energy values of edible biomass and inedible biomass (after bioprocessing). Combining several of their terms and definitions to get to the heart of the issue, we can write

$$E_e = h\upsilon_e M \tag{1}$$

$$E_i = (1 - h)\upsilon_i M \tag{2}$$

$$E_e + E_i = E_t \tag{3}$$

where

E_e, E_i = respective daily energies obtained from edible and inedible harvested biomass, kcal/person-day

E_t = total daily energy requirements, kcal/person-day

h = harvest index, g edible/g total

υ_e, υ_i = respective specific digestible energy values of edible and inedible biomass, respectively, kcal/g

M = total biomass required to be grown, g/person-day (subscripted below: $\upsilon_i = 0$, without bioprocessing; $\upsilon_i > 0$, with bioprocessing)

To compare the biomass to be grown with waste biomass processing ($M_{\upsilon_i > 0}$) to its value without such processing ($M_{\upsilon_i = 0}$), compute M for these two conditions from equations (1–3) and set the two values for M in a ratio of biomass production, r. Analytically, r is therefore

$$r \equiv \frac{M_{\upsilon_i > 0}}{M_{\upsilon_i = 0}} = \frac{h\upsilon_e}{h\upsilon_e + (1 - h)\upsilon_i} \tag{4}$$

Using the review by Westgate *et al.* for the sequence of losses that enter into the υ values, the values for υ_e and υ_i are, respectively, 3.4 and 0.4 kcal/g. The relatively low value for υ_i comes from a sequence of conversion efficiencies, which include fractional recoveries for hydrolysis, fermentation, sugars used to make edible material, and final digestibility. Although none of the terms alone is exceptionally low, their cumulative product results in the above value.

Address reprint requests to Dr. Volk at the Department of Applied Science, 26 Stuyvesant Street, New York University, New York, NY 10003

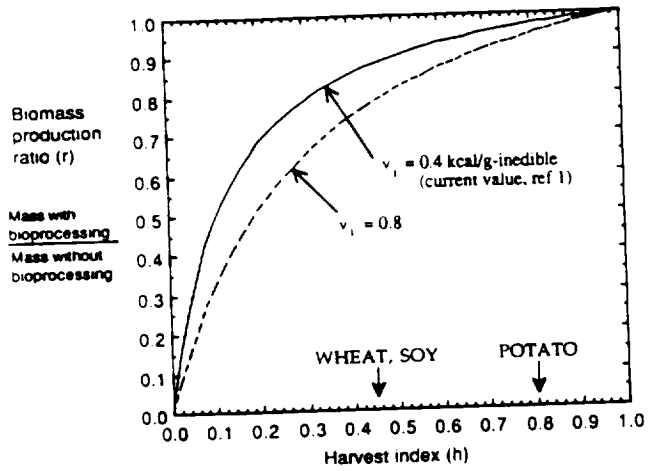

Figure 1 Plot of r as a function of h

In *Figure 1*, r is plotted as a function of h. For the case of $h = 0.2$ presented by Westgate *et al.*, $r = 0.67$ (i.e., 33 m^2/49 m^2), demonstrating the substantial savings possible with bioprocessing. For higher values of h, the value of r increases and the savings concomitantly decrease. For example, when $h = 0.45$, currently possible with soybeans and wheat in the CELSS experiments, $r = 0.87$. In this case the savings in crop biomass production by using biomass processing (which translates directly into savings in the all-important design constraints of growth area and power for lighting) is about 13%. For values of $h = 0.8$ achieved with potatoes, $r = 0.97$, implying perhaps nearly negligible savings. A second curve for r—assuming that the digestible energy potential from bioprocessing the inedible biomass could be doubled from the typical value reported by Westgate *et al.*—is shown for comparison in *Figure 1*. The values of r for soybeans-wheat and potatoes, respectively, are 0.78 and 0.94.

Harvest index is only one measure of efficacy of a crop in a CELSS and will not alone drive optimal designs; for example, nutritional values and high photosynthetic energy conversion over the entire life cycle are other important measures. However, it is clearly an ongoing research priority in the crop growth experiments to maximize the harvest index. The overall system of analysis presented by Westgate *et al.* is the kind of tool CELSS design engineers need to make tradeoffs among available options.

Although the processes that may limit its improvement are not well established, a high harvest index will always be a design goal, since, as Westgate *et al.* point out, additional equipment, volume, and power would be required for the procedures of separation, hydrolysis, and fermentation in processing the inedible biomass. The current crop values for the harvest index in *Figure 1* limit the potential savings by biomass processing. Further improvements in the harvest index that would limit these savings even more could be balanced, however, by improvements in the yields along the various steps of the bioprocessing sequence (see Ref. 1 for details of these steps). The simplified system presented here may help focus issues about options for CELSS design.

Acknowledgements

This work was supported by NASA Grant NCC2-608 to New York University.

References

1 Westgate, P., Kohlman, K., Hendrickson, R. and Ladisch, M. R. Bioprocessing in space. *Enzyme Microb. Technol.* 1992, **14**, 76–79

2 Bugbee, B. G. and Salisbury, F. B. Exploring the limits of crop productivity. *Plant Physiol.* 1988, **88**, 869–878

3 Wheeler, R. M., Mackowiak, C. L. and Sager, J. C. Proximate composition of seed and biomass from soybean plants grown at different carbon dioxide (CO_2) concentrations. *NASA Tech. Memorandum* 103496 1990, 28 pp.

4 Wheeler, R. M., Mackowiak, C. L., Sager, J. C., Knott, W. M. and Hinkle, C. R. Potato growth and yield using nutrient film technique (NFT). *Am. Potato J.* 1990, **67**, 177–187

Future Research

A proposed program of research will continue work on a progressive series of mathematical models for the CELSS hydroponic crops. The proposed research has the central *objectives* to use the experimental findings in the CELSS Program of the growth and development of candidate crops in a variety of controlled environments, for (a) systematizing crop data into engineering models that can be integrated into system-level considerations, and (b) analyzing and predicting optimal conditions for new generations of experiments.

The *approach* will be to continue the strong collaboration established over the previous years with Bruce Bugbee of Utah State University, and also to an increasingly important extent with Ray Wheeler of Kennedy Space Center. Benefits to the overall program derive from a modeler working with the experimenters, asking questions, formulating and re-formulating models, and publishing collaborative papers that organize the data into a common modeling framework. To address the most important scientific issues about the CELSS crops, the key modeling inputs are the gas exchange data from the above institutions. Gas exchange data are also now becoming available from Ames Research Center and Johnson Space Center.

These general tasks will be specifically accomplished in *two major research arenas*. First, continue development of the energy cascade as a modeling strategy that examines the components of crop growth as a sequence of conversion efficiencies. These components require ongoing analysis and prediction because they are relevant to the CELSS Program as fundamental processes of crop growth, and because they are relevant to the CELSS engineers for inclusion in general system design. Second, a new initiative will employ the relatively elaborate field crop models (Ceres-wheat, Soygro, Substor-potato, etc.). Based on the principal investigator's experience with simpler models for the CELSS crops over the previous years and collaborations with the crop researchers, these field models will be modified and used as modeling tools to predict experiments to increase yield and optimize total life cycle productivity with phasic control.